Palaeontologia Electronica
palaeo-electronica.org

The first record of *Tuarangisaurus* (Sauropterygia, Plesiosauria) from the Maastrichtian of the Lefipán Formation, Chubut, Argentina

José P. O'Gorman, Roberto A. Scasso, and Francisco A. Medina

ABSTRACT

Elasmosaurids represent the most diverse clade of plesiosaurians during the Campanian–Maastrichtian. We report a new specimen with a well-preserved cranium and postcranium from the Maastrichtian levels of the Lefipán Formation, Chubut Province, Argentina, referred to *Tuarangisaurus keyesi*. This species was previously known only from Campanian–Maastrichtian deposits of New Zealand. Phylogenetic analysis recovers *Tuarangisaurus keyesi* as the basalmost member of Weddellonectia. The hyoid apparatus is preserved and consists of a single ossified element identified as ceratobranchial I, comparable to the condition observed in other plesiosaurians. The morphology of this element is consistent with a ram-feeding strategy.

José P. O'Gorman. División Paleontología Vertebrados, Museo de La Plata, Universidad Nacional de La Plata, Paseo del Bosque s/n., B1900FWA, La Plata, Argentina and CONICET: Consejo Nacional de Investigaciones Científicas y Técnicas, Argentina. joseogorman@fcnym.unlp.edu.ar
Roberto A. Scasso. CONICET: Consejo Nacional de Investigaciones Científicas y Técnicas, Argentina. and Instituto de Geociencias Básicas, Aplicadas y Ambientales de Buenos Aires (IGeBA), Facultad de Ciencias Exactas y Naturales, Universidad de Buenos Aires. Av. Intendente Güiraldes 2160, Ciudad Universitaria, Pab. 2. rscasso@yahoo.com.ar
Francisco A. Medina. CONICET: Consejo Nacional de Investigaciones Científicas y Técnicas, Argentina. and Instituto de Geociencias Básicas, Aplicadas y Ambientales de Buenos Aires (IGeBA), Facultad de Ciencias Exactas y Naturales, Universidad de Buenos Aires. Av. Intendente Güiraldes 2160, Ciudad Universitaria, Pab. 2. famedina@gl.fcen.uba.ar

Keywords: *Tuarangisaurus keyesi*; Lefipán Formation; Elasmosauridae; Late Cretaceous

Submission: 9 January 2025. Acceptance: 10 June 2026.

Final citation: O'Gorman, José P. Scasso, Roberto A., and Medina, Francisco A. 2026. The first record of *Tuarangisaurus* (Sauropterygia, Plesiosauria) from the Maastrichtian of the Lefipán Formation, Chubut, Argentina. Palaeontologia Electronica, 29(2):a29.
https://doi.org/10.26879/1531
palaeo-electronica.org/content/2026/5903-first-record-of-tuarangisaurus-from-argentina

INTRODUCTION

Elasmosaurids are a clade of plesiosaurians that shows extreme increases in neck created by the elongation of vertebral centra and increases in cervical vertebrae account (O'Keefe and Hiller, 2006; Sachs et al., 2013). The biochron of elasmosaurids extends between the Valanginian?, Hauterivian-Maastrichtian, being one of the two, together with Polycotylidae, plesiosaurian families that reach the K/Pg boundary (Vincent et al., 2011; Benson and Druckenmiller, 2014; Fischer et al., 2018).

Elasmosaurids are, together with mosasaurs, the most frequently recorded marine reptiles in the Campanian-Maastrichtian levels of the Weddellian Province (Southern South America, Western Antarctica, and New Zealand; Zinsmeister, 1979; Hiller et al., 2005, 2017; Otero et al., 2018; O'Gorman, 2016a, b; O'Gorman et al., 2015, 2024). Recent work on Weddellian elasmosaurids has focused mainly on the skeletal morphology of aristonectines as they show extreme derived features in cranium and postcranium, except for *Alexandronectes zealandiensis,* (Cruickshank and Fordyce, 2002; Otero et al., 2016; O'Gorman, 2016a). However, non aristonectine elasmosaurids such as *Tuarangisaurus keyesi* (New Zealand, Wiffen and Moisley, 1986), *Kawanectes lafquenianus* and *Chubutinectes carmeloi* (Argentinean Patagonia, O'Gorman, 2016b; O'Gorman et al., 2023), *Vegasaurus molyi* and *Marambionectes molinai* (Antarctica, O'Gorman et al., 2015) are also present in the Weddellian Province (Welles and Gregg, 1971; Wiffen and Moisley, 1986; O'Gorman, 2012; O'Gorman et al., 2013, 2023, 2024).

The Lefipán Formation has an important historical place among the formations that have yielded plesiosaurs in Argentina as it was the first unit where aristonectines were collected (Cabrera, 1941; Gasparini et al., 2003). However, until now no non-aristonectine plesiosaurs have been described from the Lefipán Formation.

In 2003 R.A. Scasso and F.A. Medina (Facultad de Ciencias Exactas y Naturales, Universidad de Buenos Aires) collected two blocks with embedded bones and additional minor remains (numbered temporary as CPBA-V 14235, CPBA= Colección de Paleontología de la Facultad de Ciencias Exactas y Naturales) of a plesiosaurian from Estancia El Porvenir (Figure 1, Fazio et al., 2013). A subsequent prospection in the same GPS coordinates allows us to find the original location of the specimen and allows the collection of additional material from the same specimen during two fieldtrips on March 2021 and October 2021 (MPEF-PV 12001, MPEF = Museo Paleontológico Egidio Feruglio). The complete specimen, comprising the 2003 and 2021 specimens, are now registered under number MPEF-PV 12001, comprises a well-preserved skull, neck, pectoral and dorsal region, and a front limb, ribs, and gastroliths, being one of the best preserved elasmosaurids from Argentina. The aim of this contribution is to describe the new specimen, discuss its affinities and phylogenetic position, and discuss the homology of the ossified portion of the hyoid apparatus of plesiosaurians.

GEOLOGICAL SETTING

The Lefipán Formation (Turner, 1983) crops out extensively along the Valle Medio (Middle Valley) of the Chubut River (Petersen, 1946; Ruiz et al., 2005; Scasso et al., 2012) concordantly overlying the Campanian/Maastrichtian quartzose sandstones and fine conglomerates of the Paso del Sapo Formation, a unit that shows prominent exposures all over the region. MPEF-PV 12001 was found in the type locality of the Lefipán Formation (Turner, 1983), 40 km to the south of the town of Paso del Sapo (Figure 1A, B, C). A 65 m thick succession rich in marine fauna is exposed (Figure 1E, F), as it was recognized many years ago by several authors (see Turner, 1983 and references therein). The yellow to rusty brown sandstones with interbedded yellowish-brown to green mudstones of the Lefipán Formation crop out recessively above the hard sandstones of the Paso del Sapo Formation, which form cliffs along the fluvial plain of the Chubut River (Figure 1C, D, E). Locally, the Lefipán Formation is covered by deposits of an ancient (Pleistocene?) terrace from the Chubut River, or by recent debris from the basalts of the El Mirador Series (Turner, 1983) cropping out immediately to the west at the Sierra de Cutancunué. Intrusions of small basaltic bodies assigned to El Mirador Series are also observed to the southwest of the mapped area (Figure 1D). The Lefipán Formation is Maastrichtian-Danian in age (Medina et al., 1990; Olivero et al., 1990; Medina and Olivero, 1994). The mollusk fauna of Lefipán Fm. is mainly composed of oysters (Casadío, 1998), gastropods and bivalves (Olivero et al., 1990; Scasso et al., 2012) with rare cephalopods (Eubaculites); the vertebrate records are rare (Gasparini et al., 2003). The Lefipán Formation was deposited in a tide-dominated, steep-gradient, and coarse-grained deltaic system in a large embayment (Scasso et al., 2012). Mollusk faunas are abundant and macrofaunal evidence indicates that salinity was the

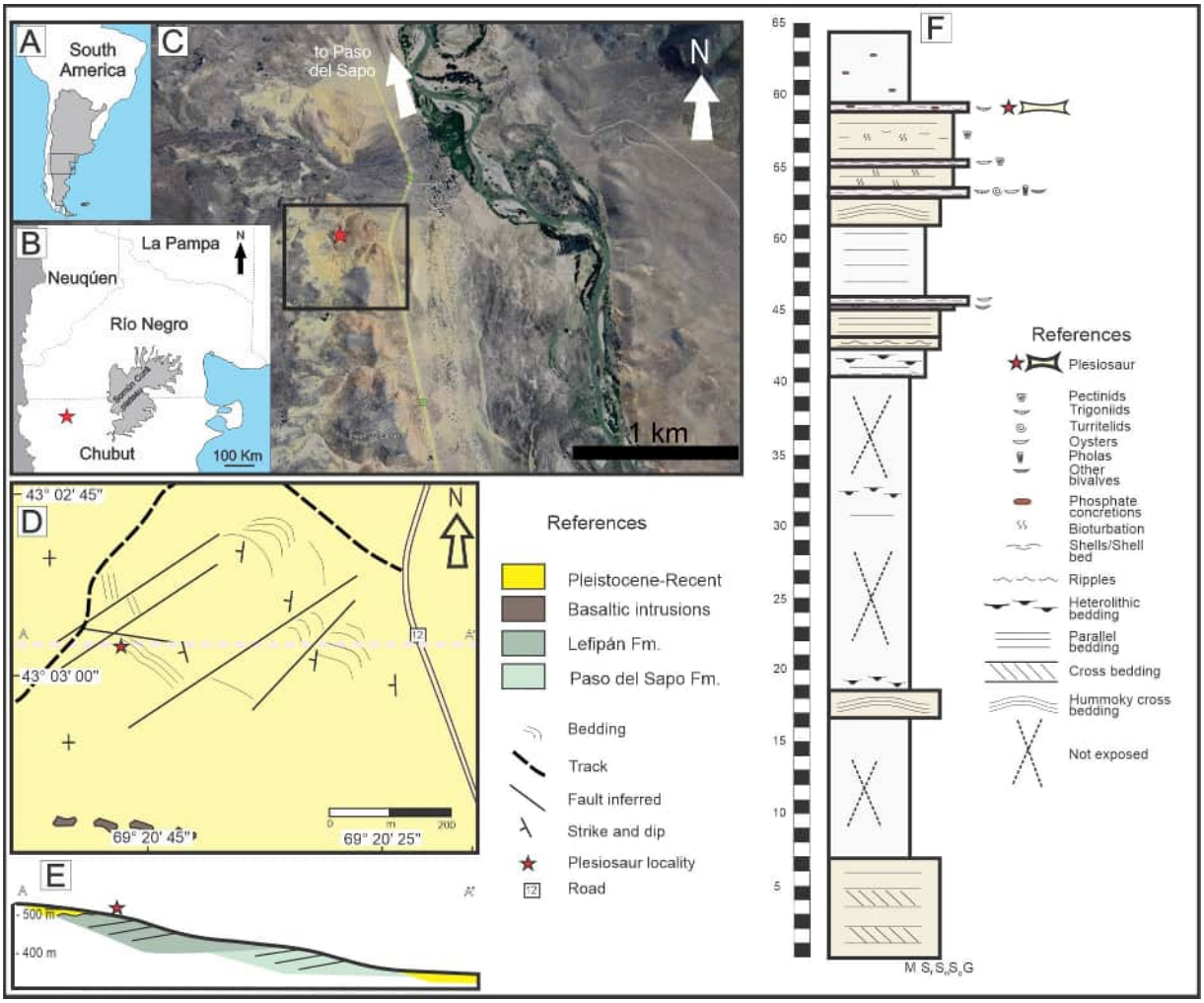

FIGURE 1. A, B, C, General maps showing the locality where MPEF-PV 12001 was collected. **D,** Sketch geological map. **E,** Geological cross section. **F,** Sedimentological section of the Lefipán Formation showing the level where MPEF-PV 12001 was collected

major factor that controlled the faunal composition and ecological structure of benthic assemblages (Scasso et al., 2012). Monospecific communities of corbiculid bivalves or oysters occurred where salinity deviated most strongly from normal marine. More diverse and complex assemblages, such as those found in the studied locality, existed in environments with a lower degree of salinity-induced stress. In these, other environmental factors such as grain size, oxygen supply, and the amount of particulate organic matter became important factors controlling the faunal associations (Scasso et al., 2012).

Institutional Abbreviations. **CPBA**, Colección de Paleontología de la Facultad de Ciencias Exactas y Naturales; **MLP,** Museo de La Plata, Buenos Aires Province, Argentina; **MPEF**, Museo paleontologico Egidio Feruglio; **NPC CD,** National Paleontological Collection, **GNS,** GNS Science, Lower Hutt; **SMUSMP**, Southern Methodist University, Shuler Museum of Paleontology, Dallas; **SMNS,** Staatliches Museum für Naturkunde, Stuttgart, Germany; **UBA,** Universidad Nacional de Buenos Aires.

Anatomical Abbreviations. al, alveoli; **ang+art**, angular + articular; **AP**, anterior process; **ataxc**, atlas-axis complex; **atna**, atlas neural arch; **atr**, atlas rib; **axna**, axis neural arch; **axr**, axis rib; **bpp**, basipterygoid process; **bat**, basioccipital tuber; **BHL**, basihial; **bo**, basioccipital; **CB**, ceratobranchial; **CHI**, ceratohyal; **caf**, carotideal foramen; **co**, coronoid; **cop**, coronoid process; **cr**, cervical rib; **cup**, cultriform process; **cv**, cervical vertebra; **dc**, distal carpal; **de**, dentary; **di**, diapophysis; **dns**, dorsal neural spine; **dr**, dorsal rib; **ds**, dorsum sellae; **dv**, dorsal vertebra; **ecp**, ectopterygoid; **ecpp**,

ectopterygoid posterior process; **epi**, epipterygoid; **epap**, epipterygoid anterior process; **exf**, exoccipital facet of the basioccipital; **exo**, exoccipital-opisthotic; **fr**, frontal; **ga**, gastralia; **gto**, gastrolith; **hu**, humerus; **hy**, hyoid element; **in**, internal naris; **int,** intermedium; **ju**, jugal; **lk**, lateral keel; **lsc**, left scapula; **Mc**, Meckelian canal; **mc**, metacarpal; **mep**, metoptica pila; **mx**, maxilla; **mxf**, maxillary foramina; **ns**, neural spine; **oc**, occipital condyle; **oaf**, occipital anterior foramen; **pak**, parasphenoid keel; **pal**, palatine; **parb**, parabasisphenoid; **pez**, prezygapophyses; **ph**, phalanges; **piv**, posterior interpterygoid vacuity; **pmx**, premaxilla; **po**, postorbital; **pop**, paraoccipital process; **poz,** postzygapophyses; **ppr,** prepectoral rib; **ppv**, prepectoral vertebrae; **pre**, prearticular; **pro**, prootic; **ps**, pisiform; **pt**, pterygoid; **ptdr**, pterygoid dorsal ridge; **ptms**, pterygoid medial sulcus; **ptpp**, pterygoid posterior process; **ptqr**, pterygoid quadrate ramus; **pv**, pectoral vertebrae; **r**, radius; **rap**, retroarticular process; **re**, radiale; **rsc**, right scapulae; **sep**, supraoccipital-epiotic; **sp**, splenial; **sq+q**, squamosal + quadrate; **st**, sella turcica; **sua**, surangular; **u**, ulna; **ue**, ulnare; **vf**, ventral foramina; **VI**, foramen for VI cranial nerve; **vn**, ventral notch; **vo**, vomer.

MATERIAL AND METHODS

Indexes

The linear measurements were obtained using a digital calliper with a precision of 0.01 mm. The indices used in the description follow those defined by Welles (1952) and include centrum length (L), the height-to-length ratio of the centrum (100 × H/L), and the breadth-to-length ratio (100 × B/L). Additionally, the breadth-to-height ratio (100 × B/H) was calculated. The vertebral length index (VLI), calculated as L divided by half the sum of height and breadth [VLI = L / (0.5 × (H + B))], was also included in the analysis. In all cases, breadth, and height measurements were taken from the posterior articular surface of the centrum.

CT scan and segmentation. CT scanning is a well-known, non-destructive technique that allows construction of a digital 3D model to view internal anatomical structures. A computer tomography (CT) scan was performed on the skull and the atlas-axis (at Instituto del Diagnóstico del Este del Chubut, Trelew City) and two main blocks and fragments that comprise the last cervical, pectoral, and a group of dorsal vertebrae (at Hospital San Martin, La Plata City). The pixel resolution is 0.39 mm, other data of the two CT are given in Table 1. Data were collected from the scanner in DICOM format and processed using the editing tools for segmentation of the InVesalius 3.0 free software (Martins et al., 2007).

Phylogenetic Analysis

The data set is based on those of Benson and Druckenmiller (2014) and Serratos et al. (2017), modified by O'Gorman (2019) and O'Gorman et al. (2021, 2023, 2024) with the addition of the polycotylids from the data set of Fischer et al. (2018) and three characters and scorings from Morgan and O'Keefe (2019). Additionally, the scorings of the new specimen were added. The data set includes *Tuarangisaurus keyesi* (holotype NPC CD 425 and NPC CD 426) and the specimen (MPEF-PV 12001) as separate scorings (Supplementary Material 1) and other scoring with combined scores (NPC CD 425 + NPC CD 426 + MPEF-PV 12001, Supplementary Material 2). This adds 43 new scores (14.8 % additional scores) to *T. keyesi.* The Character 109 was modified ectopterygoid/pterygoid boss/flange by the addition of state (3); ventrally deflected posterior margin forms posteroventral long and pointed projections that is located ventrally to the plane of palatine.

The complete data sets were analyzed with the TNT 1.5 software package (Goloboff and Catalano, 2016). All characters were considered unordered except for Ch. 155 (modified by O'Gorman, 2019). The analysis was carried out using New Technology (sectorial search, ratchet, drift, tree fusing with the default settings) with 10,000 replicates. The MPTs obtained were then used as the starting point to perform TBR swapping. Bremer Support (Bremer, 1994) values were calculated using TNT for some nodes to test clade robustness.

TABLE 1. CT scans setting and used CT devices.

Material	matrix size/#slices/thickness	USED CT Device
MPEF-PV 12001 Skull and atlas-axis complex	512x512/ 504 slices/0.5 mm	TOSHIBA Aquilion Lightning (TSX-035A)
MPEF-PV 12001 Cervical and dorsal region	512x512 /2534 slices/0.5 mm	CANON Aquilion Prime SP

SYSTEMATIC PALEONTOLOGY

Subclass SAUROPTERYGIA Owen, 1860
Order PLESIOSAURIA de Blainville, 1835
Superfamily PLESIOSAUROIDEA Welles, 1943
Family ELASMOSAURIDAE Cope, 1869
Genus *TUARANGISAURUS* Wiffen and Moisley, 1986

Type species. *Tuarangisaurus keyesi* Wiffen and Moisley, 1986 by original designation.

Tuarangisaurus keyesi
Wiffen and Moisley, 1986
Figures 2–16

Emended diagnosis. An elasmosaurid characterized by one autapomorphy: ectopterygoid with large boss on the ventral surface that end in a ventro-caudally directed long process that reaches the middle of the posterior interpterygoid vacuity. The following features also allow differentiation of *Tuarangisaurus keyesi* from other elasmosaurids: 15/16 maxillary alveoli, differing from aristonectines; no caniniform teeth, differing from aristonectines; ventral margin of the orbit convex and formed mostly by the maxilla, differing from *Eromangasaurus australis* and *Futabasaurus suzukii*; absence of parietal foramen, differing from *Callawayasaurus colombiensis*; anterior ramus of pterygoid overlaps posterior half of vomer; absence of posterior interpterygoid symphysis; parasphenoid with ventral keel; quadrate ramus of the pterygoid plate like and projects from the lateral surface of pterygoid, paraoccipital process long and compressed articulating with squamosal and pterygoid; twenty-one/twenty three dentary alveoli; high triangular coronoid process, differing from *C. colombiensis* and *Zarafasaura oceanis*; atlas rib as long as the axis rib; axis rib dorso-ventrally compressed, differing from *Vegasaurus molyi*; axis neural spine ending anterior to the postzygapophyses, differing from *Thalassomedon haningtoni.* Atlas-axis complex with heart shaped atlantal cup differing from *Aristonectes parvidens, Wunyelfia maulensis,* and *Marambionectes molinai;* and with low rounded ventral ridge differing from *Libonectes morgani*. Cervical vertebrae with lateral keel differing from *Aristonectes parvidens* and *Nakonanectes bradti*; cervical articular faces with ventral notch until the caudal-most cervical, differing from *C. colombiensis* and *Z. oceanis* and *Traskasaura sandrae.* Anterior margin of neural spine of anterior cervicals curved caudally. Posterior cervical neural spines caudally inclined differing from *F. suzukii; Kawanectes lafquenianus* and *A. quiriquinensis.* Two pectoral vertebrae; scapula with medial symphysis along ventral plates; epipodial elements wider than long; epipodial foramen; metatarsal V completely shifted to the carpal row; accessory ossicle between ulna and ulnare.

Holotype. NPC CD 425 skull and NPC CD 426, fused atlas-axis and seven successive cervical vertebrae, left angular quadrate, and squamosal.

Type locality and horizon. Mangahouanga Stream, a northern tributary of Te Hoe River, inland Hawke's Bay, New Zealand Fossil Record File number V19/f6909 (Figure 1). Maungataniwha Sandstone Member of the Tahora Formation. Upper Campanian-lower Maastrichtian, *Isabelidinium pellucidum* Zone (Vajda and Raine, 2010).

Referred material. MPEF-PV 12001, skull, and mandible (Figures 2–9); cervical vertebrae, two pectoral vertebrae, eight dorsal vertebrae, ribs, and a scapula representing by a natural moulds, (Figures 10–15) humerus, radius, ulna, carpus, phalanges (Figure 16), and gastroliths (Figures 12, 13).

Locality and horizon. Puesto Ybarra Locality, Estancia El Porvenir, middle Chubut River (Figure 1C), northwestern Chubut Province, Patagonia, Argentina (Cabrera, 1941); Lefipán Formation, Maastrichtian (Lesta and Ferello, 1972; Page et al., 1999).

Remarks. MPEF-PV 12001 shows an ectopterygoid with large boss on the ventral surface that ends in a ventro-caudally directed long process that reaches the middle of the posterior pterygoid vacuity, an autapomorphy of *T. keyesi,* and therefore it is referred to this species. However, there are some differences with the holotype that are interpreted as related to the juvenile condition (See Discussion).

DESCRIPTION

General Description of (MPEF-PV 12001)

The specimens were collected semi-articulated during two different field seasons. In 2003 two blocks were collected comprising the five caudal-most cervicals, two pectorals and two dorsal vertebrae (Figure 13) and a second block containing a sector or six dorsal vertebrae (numbered I to VI) and three additional middle cervical were also collected at that time. (Figures 11F-H, 14). A second fieldwork occurred in 2021 allowed the collection of other parts of the same specimen, comprising skull, mandible and anterior cervical articulated, three sectors of cervical region articulated and partially preserved anterior limb fragments of the girdles. The skull is almost complete, lacking only the premaxilla, and elements of the skull roof except

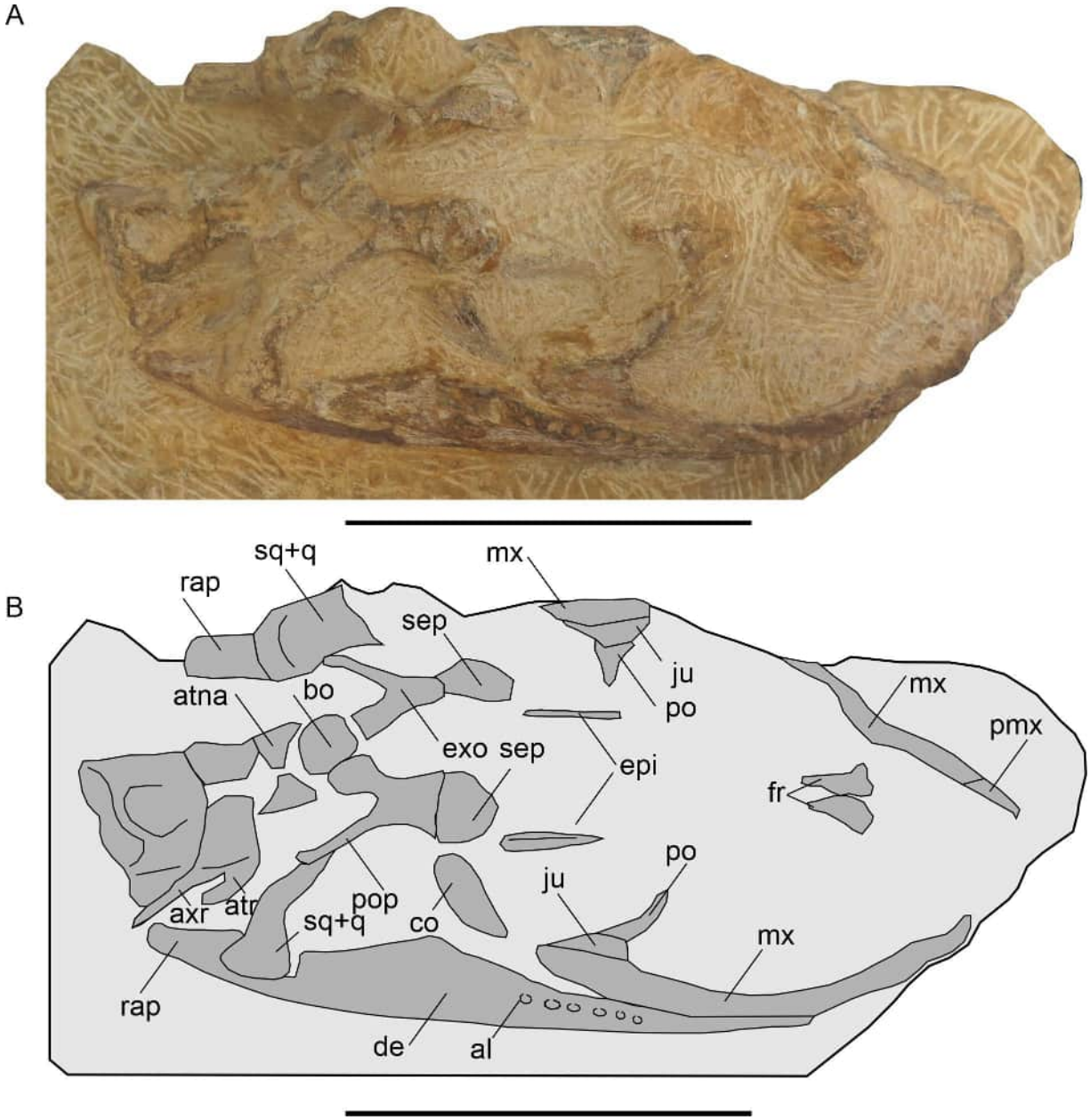

FIGURE 2. *Tuarangisaurus keyesi* (MPEF-PV 12001). Skull and mandible in dorsal view. **A**, photography and **B**, diagram. Scale bar equals 100 mm.

for part of the frontals that are partially preserved. Additionally, the mandible and hyoid apparatus were recovered in natural position, although the mandible lacks a well preserved mandibular symphysis.

Skull Anatomy

General description. The skull preserves the mandible, most of the upper jaw, basicranium, and palate in natural position. All elements are articulated and only slightly dorso-ventrally compressed (Figures 2-5). The hyoid apparatus is also preserved and located at the middle level of the posterior part of the palate and shows an almost symmetrical position (Figure 5C).

Craniofacial Skeleton

Premaxilla. Only a small section of the left premaxilla is preserved (Figures 2, 3, 4), preserving two alveoli. The premaxilla-maxilla suture runs dorso-caudally.

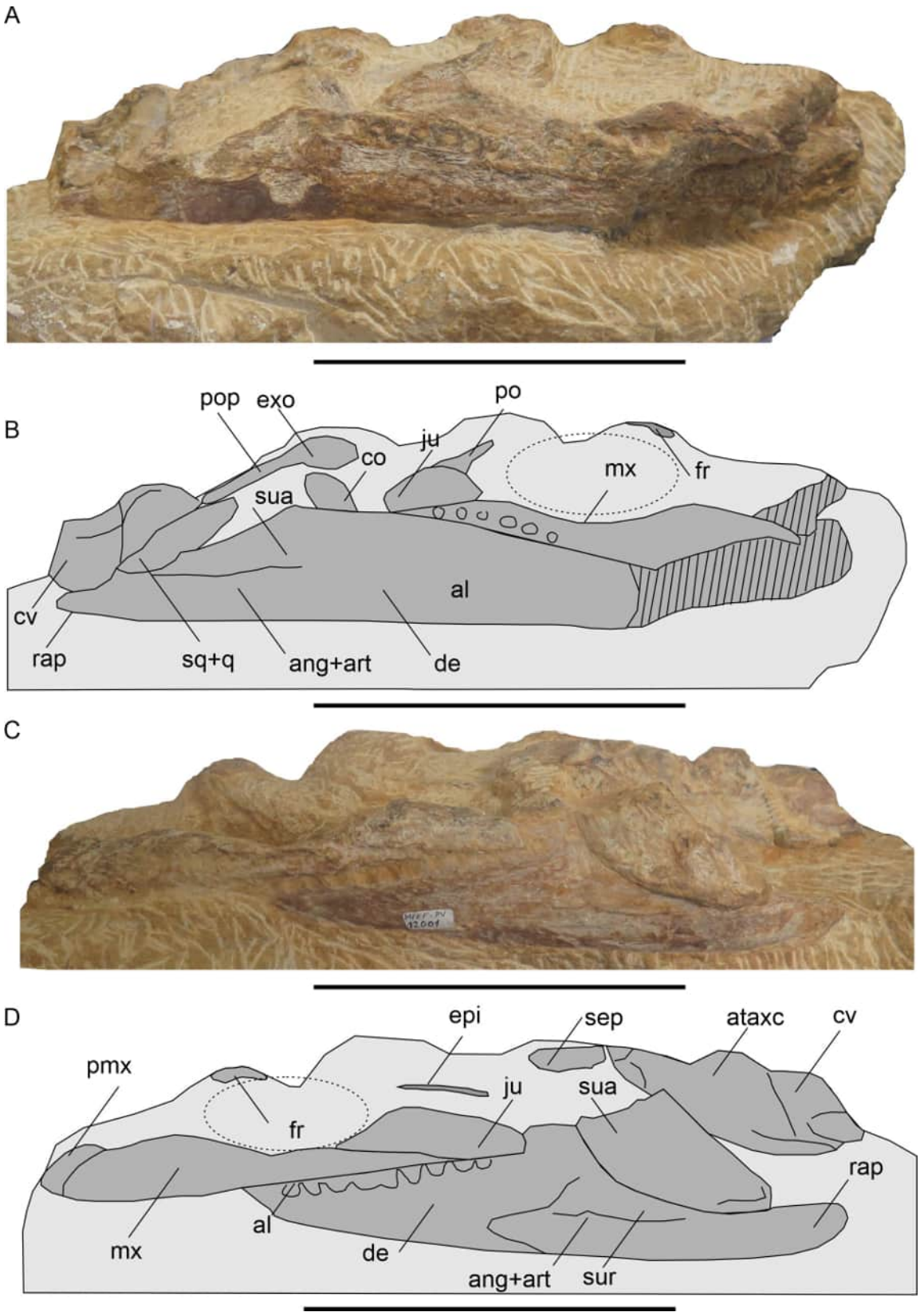

FIGURE 3. *Tuarangisaurus keyesi* (MPEF-PV 12001). **A-B,** Skull and mandible in right lateral view. **A**, photography and **B**, diagram. **C-D,** Skull and mandible in left lateral view. **C,** photography and **D,** diagram. Dotted line indicates orbit. Scale bar equals 100 mm.

Maxilla. The maxilla bears about 16 alveoli. The maxilla forms the anteroventral margin of the orbit, which is slightly convex (Figure 4C), as is recorded in other elasmosaurids such as *Hydrotherosaurus alexandrae, Thalassomedon haningtoni,* and *Kaiwhekea katiki* (Welles, 1943; Carpenter, 1999; Benson and Druckenmiller, 2014). The maxilla also bears a line of foramina (four at the level of the orbit and three additionally anterior to the orbit) located between the ventral orbital margin and the alveolar margin (Figure 4C). The maxilla-jugal suture is long posteroventrally and almost horizontally directed (Figure 4C) as in other elasmosaurid except for *Zarafasaura oceanis*, where the suture is shorter and almost dorso-ventrally directed (Vincent et al., 2011).

Frontal. Only parts of both frontals are preserved located in natural position and meeting in the midline, although it is possible that the medial area of both be covered by a process of the premaxilla (Figures 2, 3). Ventrally it preserves paired projections that limit the olfactory sulcus that enclosed the olfactory tract.

Jugal: only a small portion is preserved on the dorsal margin of the maxilla (Figure 4C, B).

Postorbital. only a small portion of both postorbitals are preserved, which delineates the caudal margin of the orbit, they are high and gracile (Figure 4B).

Squamosal + quadrate. Only the quadrate ramus and part of the temporal rami of squamosal is preserved, it covers the quadrate medially and laterally, by a medial and a lateral process (Figures 4, 5A). The lateral process reaches a more ventral level than the medial one. The position of the medial symphysis between both squamosals (not preserved) is located at the level of the supraoccipital, the squamosals form a V-shaped embayment caudal margin (angle less than 90°).

Braincase

Basioccipital. The dorsal surface of the basioccipital bears two poorly defined exoccipital facets and the floor of the foramen magnum (Figure 6D). Its entire dorsal surface is strongly inclined anteriorly (Figure 6A). The basioccipital projects laterally, generating a lateral step forming the basioccipital tubers (Figures 4A, B; 5A, 6). The occipital condyle is rounded and wider than tall. No condylar neck is present on the dorsal or ventral surfaces. The basioccipital ventral process is a step small and rounded (Figures 5A, 6B). The anterior surface of the basioccipital bears a small conical projection and is pierced by a circular foramen. The limit between the basioccipital and the basisphenoid shows a space that was occupied by chondral tissue.

Parabasisphenoid complex. The parasphenoid and basisphenoid are completely fused, forming a parabasisphenoid complex. The ventral surface of the parabasisphenoid, formed by the parasphenoid bears a medial high keel (Figures 5A, B, C; 6A, C, D) that ends cranially at the level of the cultriform process (Figure 4A). The cultriform process is dorso-ventrally compressed, diamond-shaped in ventral view, and ventrally covered by the pterygoid (Figures 4A, 6C, D). Caudally the parasphenoid covers ventrally the basioccipital to the level of the base of the occipital condyle, ending in two lateral projections and a medial projection that bears a high ventral medial keel (Figure 5C, D).

The lateral surface of the basisphenoid forms the basipterygoid process that contacts with the pterygoids (Figure 6D) and limit laterally a longitudinal groove. The internal carotid foramen, although it is only well reconstructed on the left side, are located posterior to the basipterygoid process (Figure 6D). The foramen enters in a medial direction, directly to the sella turcica (Figure 6D) without running inside the bone, differing from the holotype of *Tuarangisaurus keyesi* (O'Gorman et al., 2017: fig. E). There are paired canals for VI cranial nerve (Figure 6C). The anterior end of the floor of the sella turcica is laterally concave and ends in a notch located in the anterior margin of the sella turcica (Figure 6D) The lateral margins of the sella turcica bear one lateral metoptic pila on each side (Figure 6D).

Epipterygoid. The epipterygoids are thin bones located dorsally to the pterygoid. The epipterygoids bear a marked anterior process located on their dorsal margin. The epipterygoid borders laterally with a space formed by a deep groove on the lateral surface of the basipterygoid process, likely for the passage of the V1 branch of the trigeminal nerve and the VI nerve (Figure 6C).

Exoccipital-opisthotics. Both exoccipital-opisthotics are preserved in natural position. The exoccipital and opisthotic are fused, and no suture could be detected, a condition observed in other plesiosaurians (Andrews, 1913; Sato et al., 2011; Ketchum and Benson, 2011). The paraoccipital processes are relatively long and slender (23 mm in length and 4 mm in dorso-ventral width) and articulate ventrally with pterygoid and distally with squamosal. No foramen for cranial nerves could be segmented on the exoccipital-opisthotics.

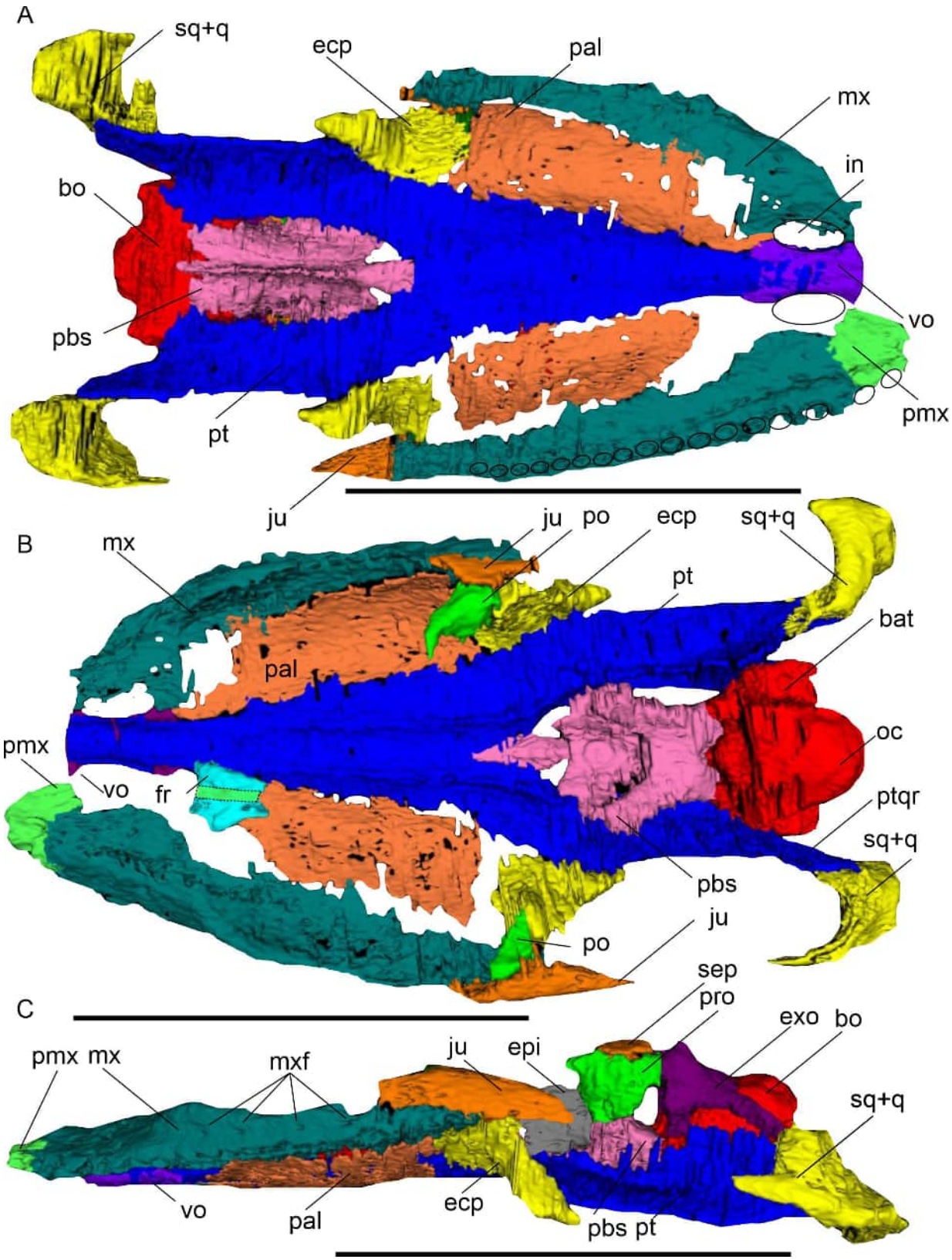

FIGURE 4. *Tuarangisaurus keyesi* (MPEF-PV 12001). Skull segmentation (**A-B,** otic bones removed). Skull in **A**, dorsal and **B**, ventral view. **C**, skull in left lateral view. Scale bar equals 100 mm.

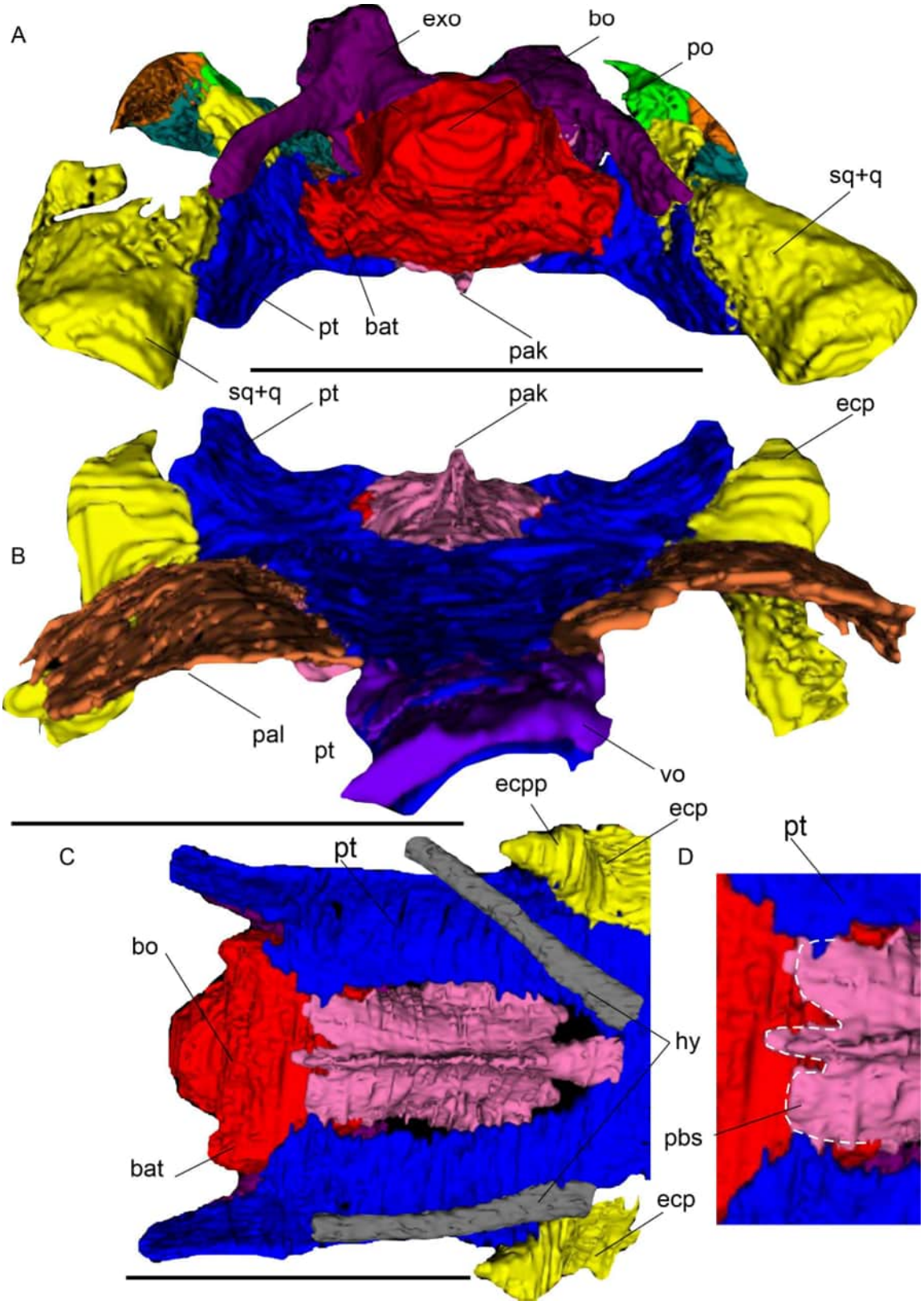

FIGURE 5. *Tuarangisaurus keyesi* (MPEF-PV 12001). Skull segmentation. **A-B** (otic bones removed). Skull in **A**, occipital and **B**, anterior, views. **C**, posterior palate detail and **D** detail of parabasisphenoid posterior end.. Scale bar equals 50 mm.

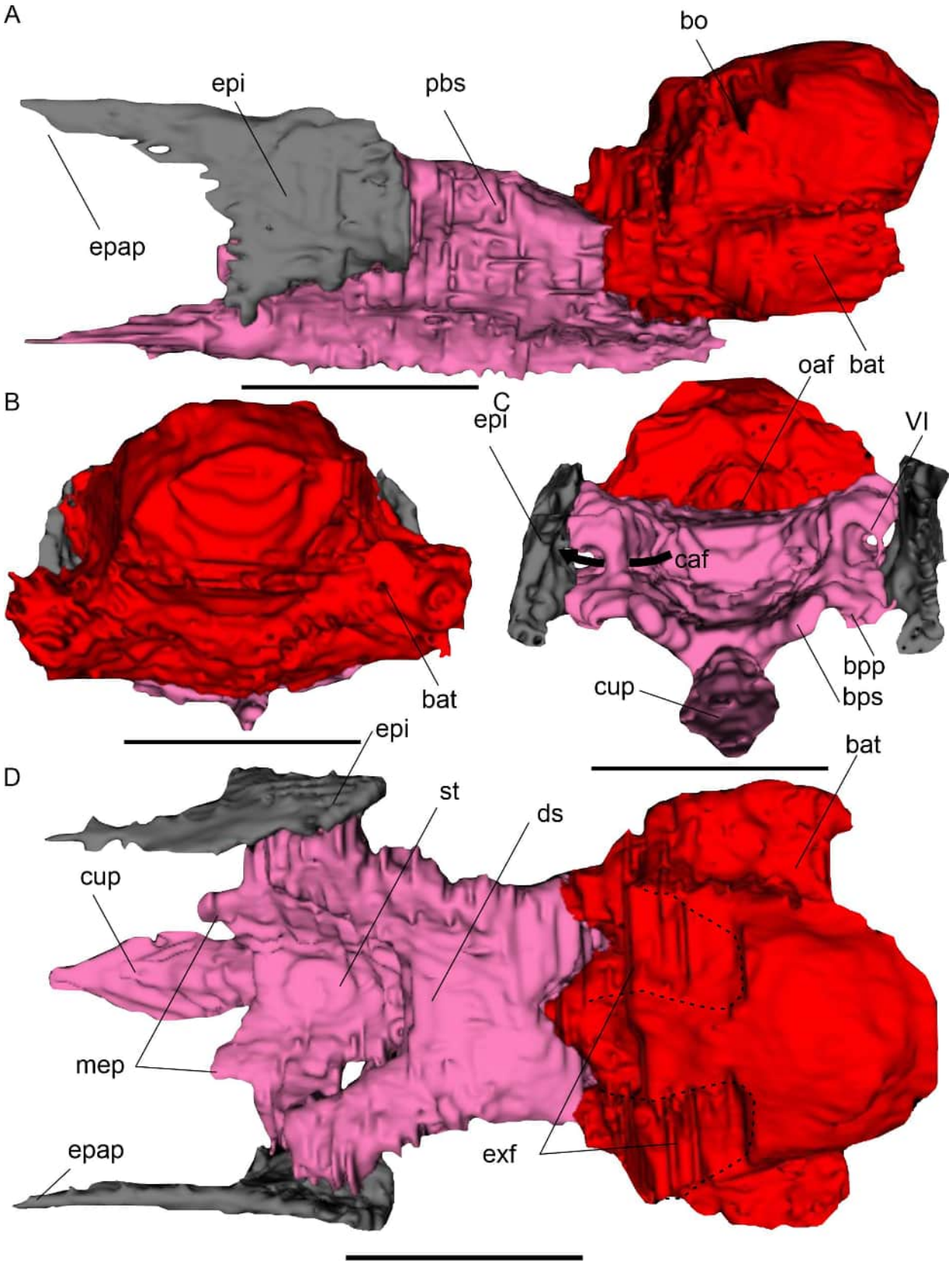

FIGURE 6. *Tuarangisaurus keyesi* (MPEF-PV 12001). Basioccipital, basiparasphenoid, epipterygoids articulated in **A**, left lateral, **B**, occipital, **C**, anterior and **D**, dorsal view. Scale bar equals 20 mm.

Prootic. Preserved, articulated with the basisphenoid and opisthotic and dorsally with the supraoccipital-epiotic. The prootic forms the posterior border to the fenestra ovalis limiting it by an anterior ventral process.

Supraoccipital-epiotic. The supraoccipital-epiotic are badly preserved, preserving only the parts articulating with the exoccipitals-opisthotic (Figures 4C, 7).

Palate

Vomer. The vomer is partially preserved, lacking its anterior end. It underlapped the anterior end of the anterior process of pterygoid. The middle part of the vomer narrows encompassing the formation of the internal nares (Figures 4A, B; 5B).

Internal nares. The internal nares are elliptical and anteropoteriorly elongated. They are delineated laterally by the maxilla and medially by the vomer. It is not clear if the palatine participates in a small lateromedial area (Figure 4A).

Palatine. The palatines are mostly flat plates that articulates laterally to the maxilla, medially to the pterygoid and caudally with the ectopterygoid. In the caudal limit the palatine limit with the anterior end of the ectopterygoid (Figures 4A, B; 5B).

Pterygoid. The pterygoids form a large plate that connects all elements of the palate. It could be divided into an anterior process, a central plate, the lateral plates (the portion of pterygoid located lateral to the posterior interpterygoid vacuity), and the quadrate rami (Figure 4A, B). The anterior process is long; its dorsal surface is concave, forming a shallow longitudinal groove (Figures 4A, B; 8A). The anterior process overlaps anteriorly the caudal end of the vomer (Figure 5B). No anterior interpterygoid fenestra is present (Figure 4). The central plate of the pterygoid covers ventrally the anterior end of the cultriform process of the parasphenoid. Caudally the pterygoid expands into the lateral rectangular plates that limit medially the posterior interpterygoid vacuity that shows a length/width ratio of about 1/2 (23 mm wide/40 mm long). Caudally the medial margin of the lateral plates forms small projections that embrace the basioccipital ventrally but no posterior interpterygoid symphysis is present (Figures 4A, B; 5A). The ventral surface of the lateral plates is lateromedially concave with a lateral margin located more ventrally than the medial one, forming a lateral ridge-like margin (Figures 5B; 8B). The quadrate ramus of the pterygoid is plate like and is continuous with the lateral ramus, differing from *Callawayasaurus colombiensis* and *Libonectes morgani* (Welles, 1962; Carpenter, 1997) where a small step is present. Dorsally the lateral plates bear an anteroposterior vertical wall that merge with the quadrate ramus of the pterygoid (Figure 8A) as the latter change its direction to dorso-ventrally directed anterior to the contact with the quadrate. There is space between the quadrate ramus of pterygoid and the basioccipital tubers (Figure 5A).

Ectopterygoid. The ectopterygoid limit anteriorly the subtemporal fenestra and articulate anteriorly with the palatine and medially with the pterygoid and laterally with the maxilla (Figure 5). The anterior end is flat and expanded with an anterior convex margin (Figure 8A, B). The ventral surface bears a large dome that projects ventro-caudally parallel to the lateral margin of the lateral plates of pterygoid ending in a pointed distal end (Figure 8B).

Mandible

Dentary. In both dentaries, the anterior portion is missing, and the mandibular symphysis is completely absent. The dentary bears approximately 21 alveoli, however as the mandibular symphysis is not preserved the number is at least 23. The dentary shows a Meckelian canal that runs anteriorly until the anteriormost preserved portion (Figure 9C).

Coronoid. The coronoid is triangular shaped with a wide base (36 mm wide, 27 mm high) that expands in a cranio-caudally direction on the medial view of mandible, being the anterior expansion taller than the posterior one (Figure 9B, D). The coronoid process is high and ends in a pointed tip (Figure 9D). The anterior margin is gently concave and inclined anteriorly while the caudal margin is strongly concave, making the distal end caudally directed (Figure 9D).

Prearticular. The prearticular is a small flat bone located caudally to the splenial (Figure 9B).

Surangular. The surangular articulates anteriorly with the dentary and ventrally with the angular, its dorsally end is pointed but does not participate in the coronoid process (Figure 9A).

Articular. The retroarticular is caudally directed with a gentle dorsal inflexion of the ventral margin and a dorsal surface medially directed (Figure 9A). The glenoid cavity is slightly shorter than the retroarticular process (retroarticular process length 17 mm/glenoid length 13 mm).

Hyoid. A pair of ceratobranchials I (see discussion) is preserved (Figures 5C, 9C), measuring 45 mm in length and 4.5 mm in minimum width. The

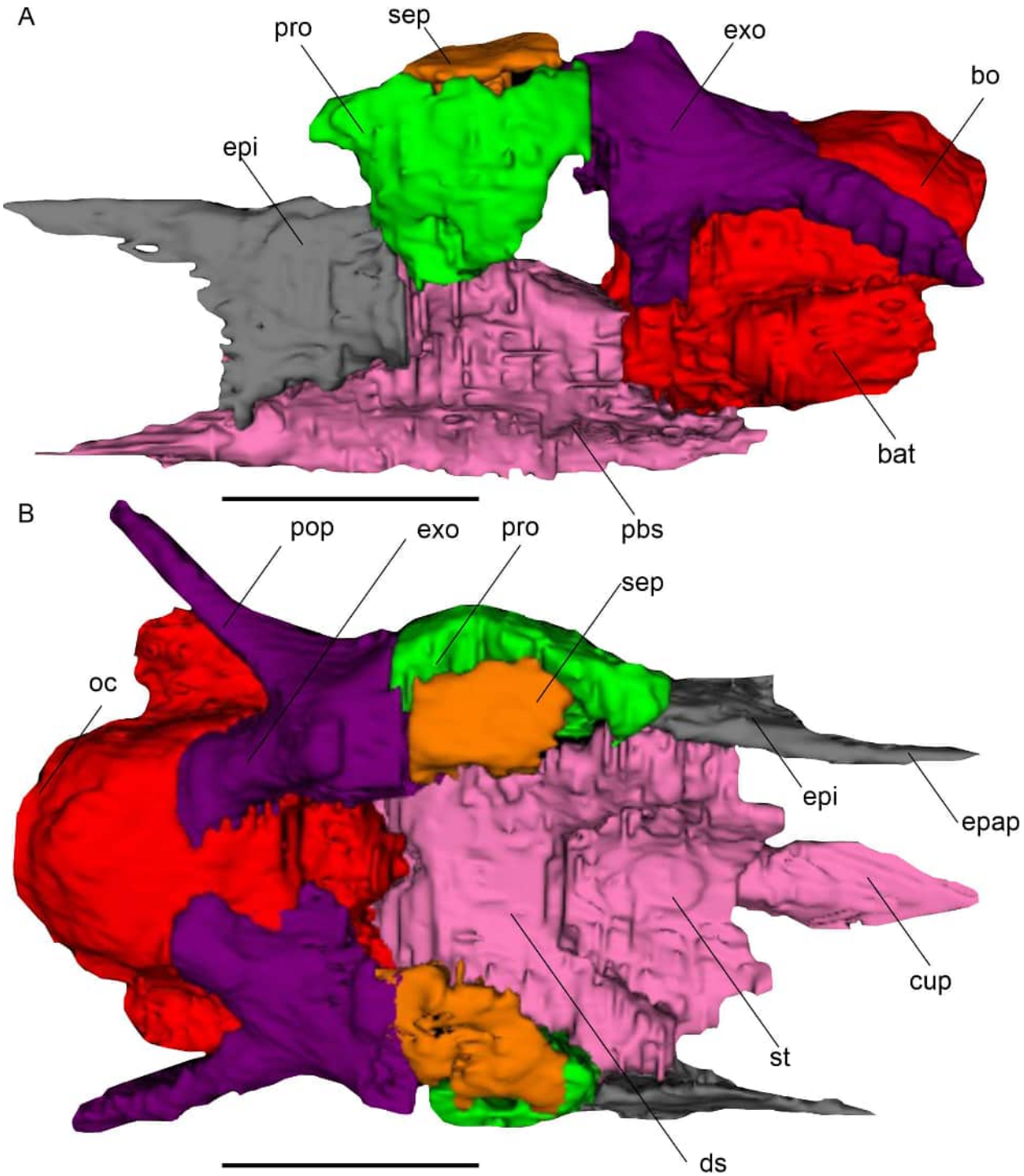

FIGURE 7. *Tuarangisaurus keyesi* (MPEF-PV 12001). Braincase in **A**, left lateral and **B**, dorsal views. Scale bar equals 20 mm.

ceratobranchials I bones show a slightly curved axis and a distal small expansion.

Vertebral Column

Cervical region. The atlas axis complex is well preserved although the dorsal part of the neural arch is missing (Figure 10A, B). The atlantal cup is heart shaped in anterior view. Ventrally there is a low and rounded ventral hypapophysis. The articular face of the axis is rectangular shaped (Figure 11B). The axis rib is dorso-ventral flat and is pre-

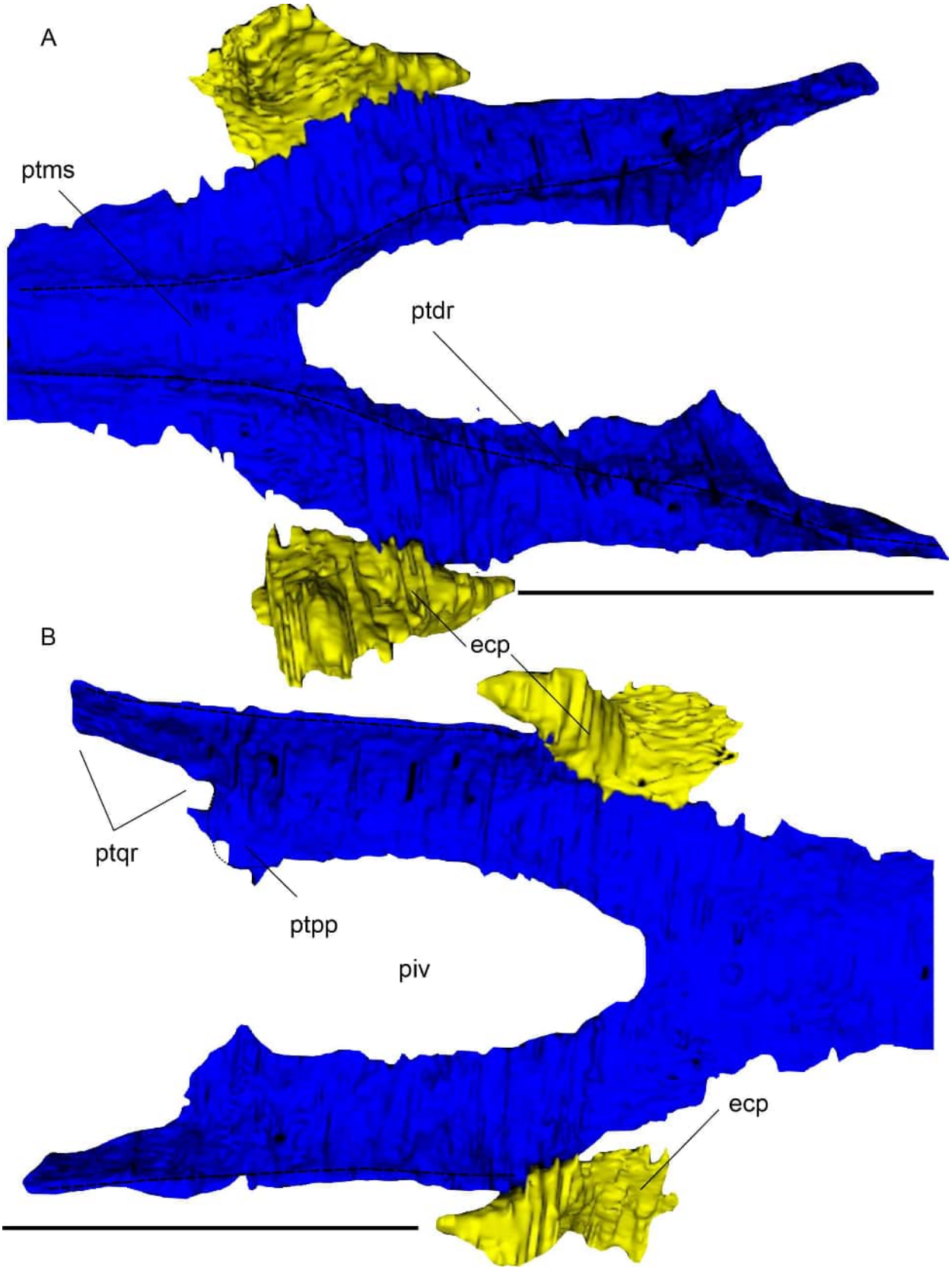

FIGURE 8. *Tuarangisaurus keyesi* (MPEF-PV 12001). Pterygoid and ectopterygoid articulated. **A**, dorsal and **B**, ventral views. Scale bar equals 50 mm.

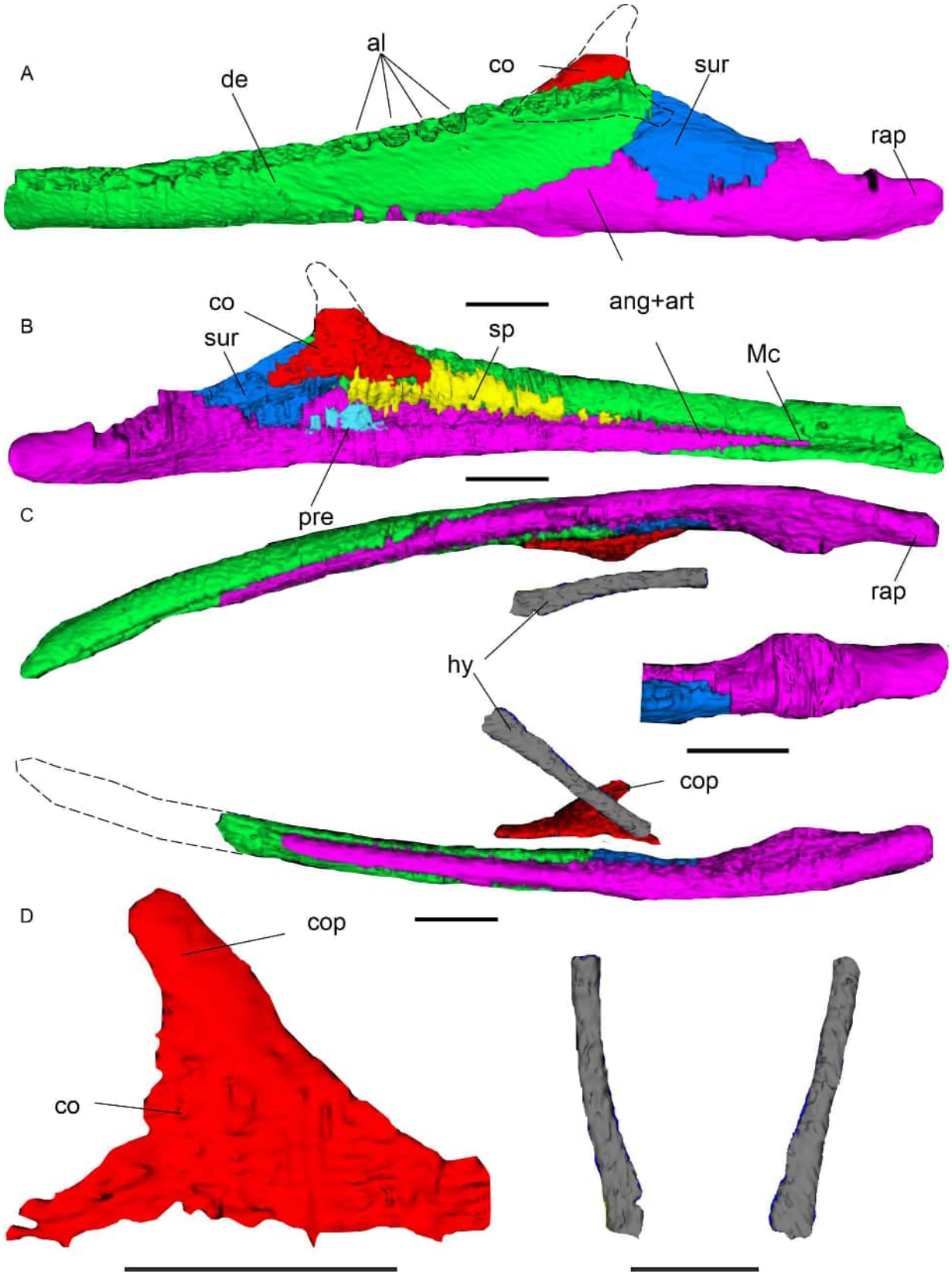

FIGURE 9. *Tuarangisaurus keyesi* (MPEF-PV 12001). Mandible. **A**, left mandibular ramus in lateral view; **B**, right mandibular ramus in medial view; **C**, both mandibular ramus in dorsal view. **D**, left coronoid in medial view. Scale bar equals 20 mm.

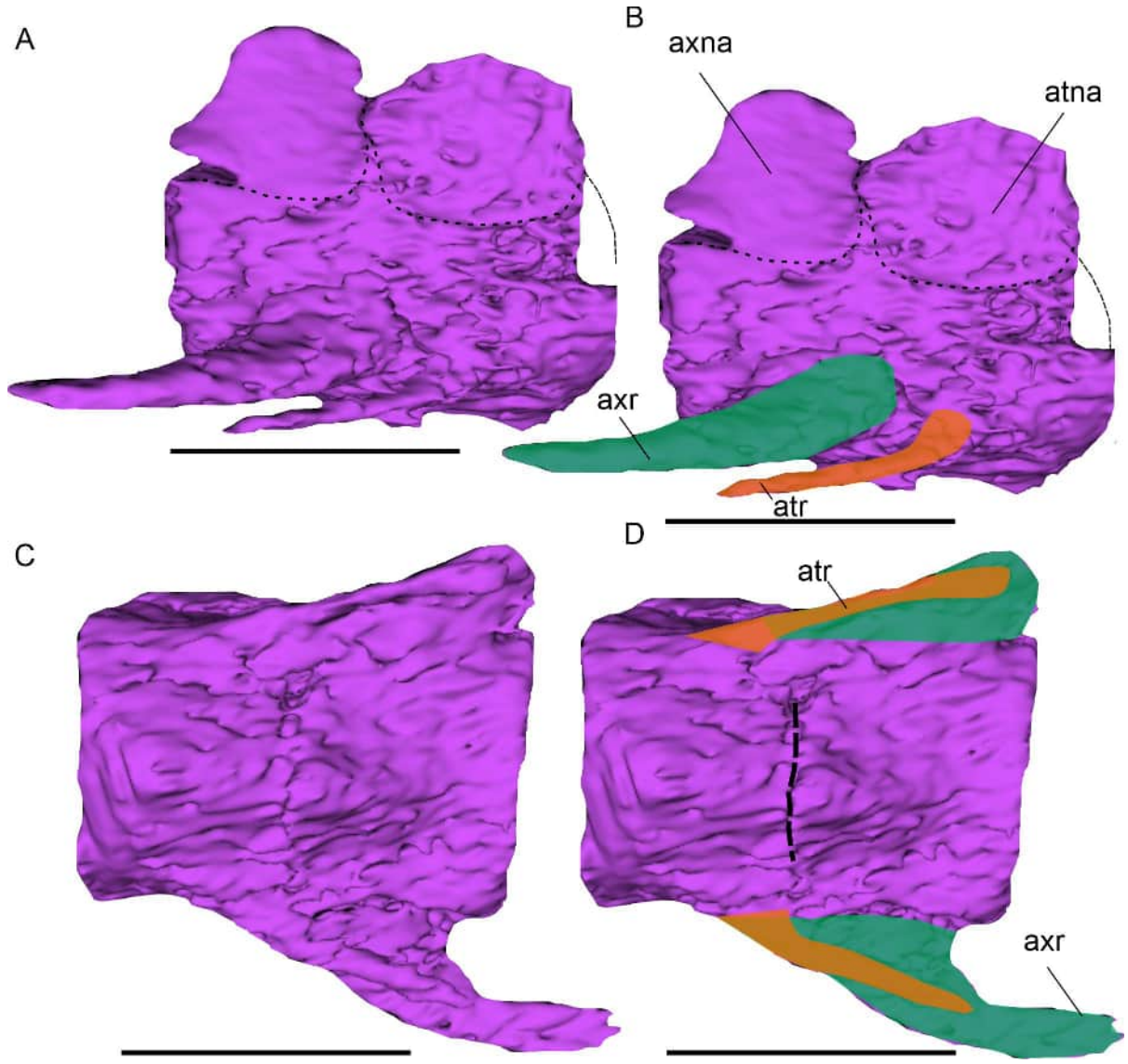

FIGURE 10. *Tuarangisaurus keyesi* (MPEF-PV 12001). Atlas-Axis complex in **A**, **B**, right lateral and **C**, **D**, ventral view. **B**, **C**, atlas ribs (orange) and axis ribs (green) indicated. Scale bar equals 20 mm.

ceded by a long and thin atlas rib or rib-like process (Figure 10C, D).

There are 45 post-axial cervical vertebrae. The vertebral bodies are as longer than high and wider than long in the anterior cervical vertebrae (Table 2). There is a lateral keel, at least since the thirteenth to the twenty-seventh vertebrae. The articular face shows a ventral notch giving a bilobate outline that is present at least from the eleventh vertebrae to the caudalmost cervical vertebrae (Figure 11D, I). The neurocentral suture is open and V-shaped (Figures 11, 12). Ventrally the vertebral centrum is pierced by two foramina. The neural spine of the anterior cervical (15th-16th) are rounded and slightly caudally expanded, but the middle posterior and posterior cervical the neural spine is slightly caudally inclined (Figure 12A, C). The prezygapophysia are medially inclined and fused in midline, postzygapophyses are also fused in midline.

Pectoral region. There are two pectoral vertebrae. The first one shows the transverse process formed by one-third of the neural arch and two-thirds from the cervical centra. The first pectoral bears five ventral foramina. The neural spine is rectangular shaped and caudally inclined.

Dorsal Region

There are six dorsal vertebrae preserved. The dorsal centra are as high as long as and wider than

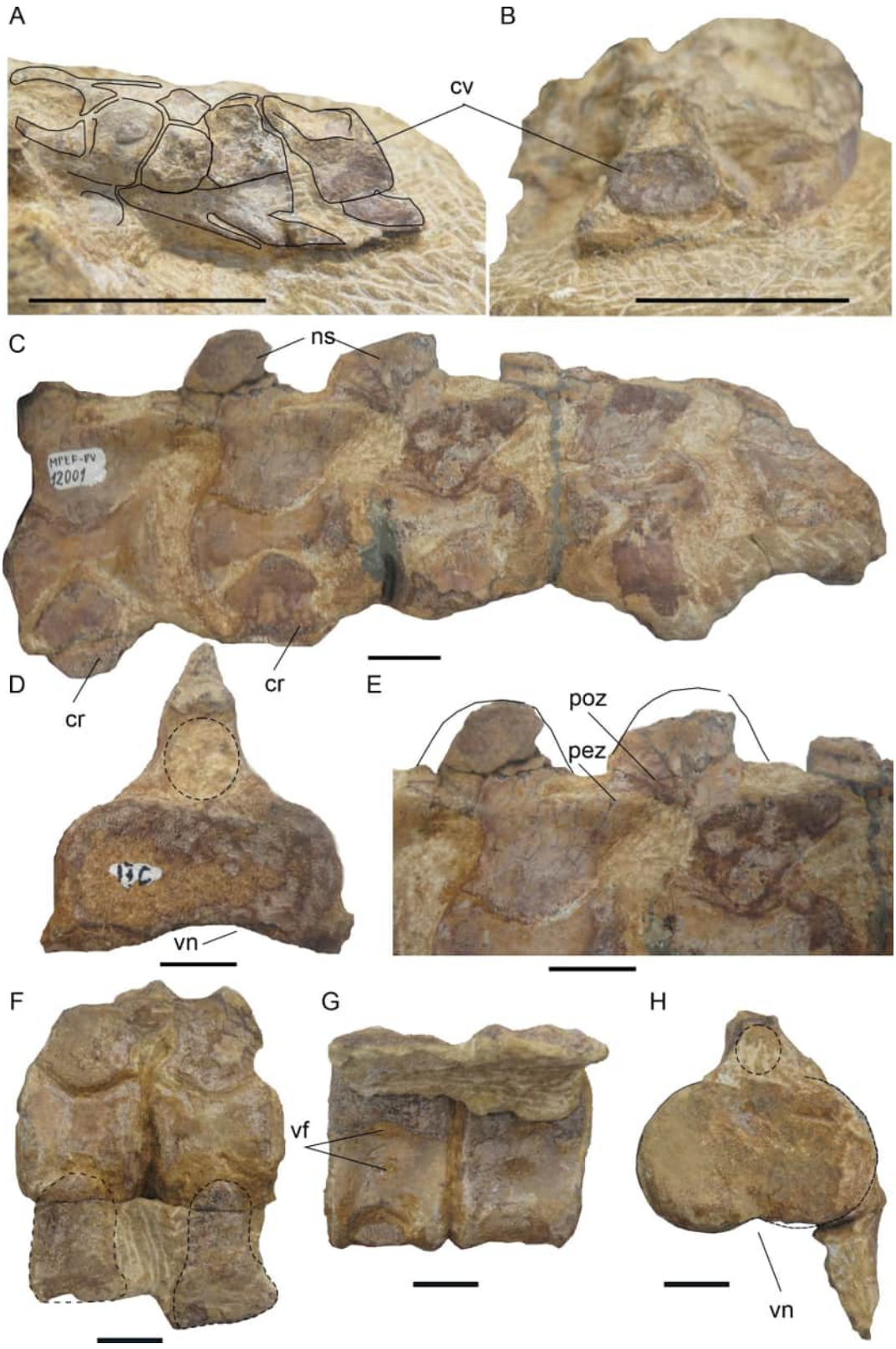

FIGURE 11. *Tuarangisaurus keyesi* (MPEF-PV 12001). **A**, Atlas-Axis complex and 3rd cervical in lateral view. **B**, 3rd cervical in posterior view. **C-E,** Anterior cervicals in **C**, right lateral view. **D**, posterior and **E,** detail of neural spines. **F-H,** middle cervical vertebrae in **F,** right lateral, **G**, ventral and **H**, posterior. Scale bar equals **A**, **B** = 50 mm; **C-H,** 20 mm.

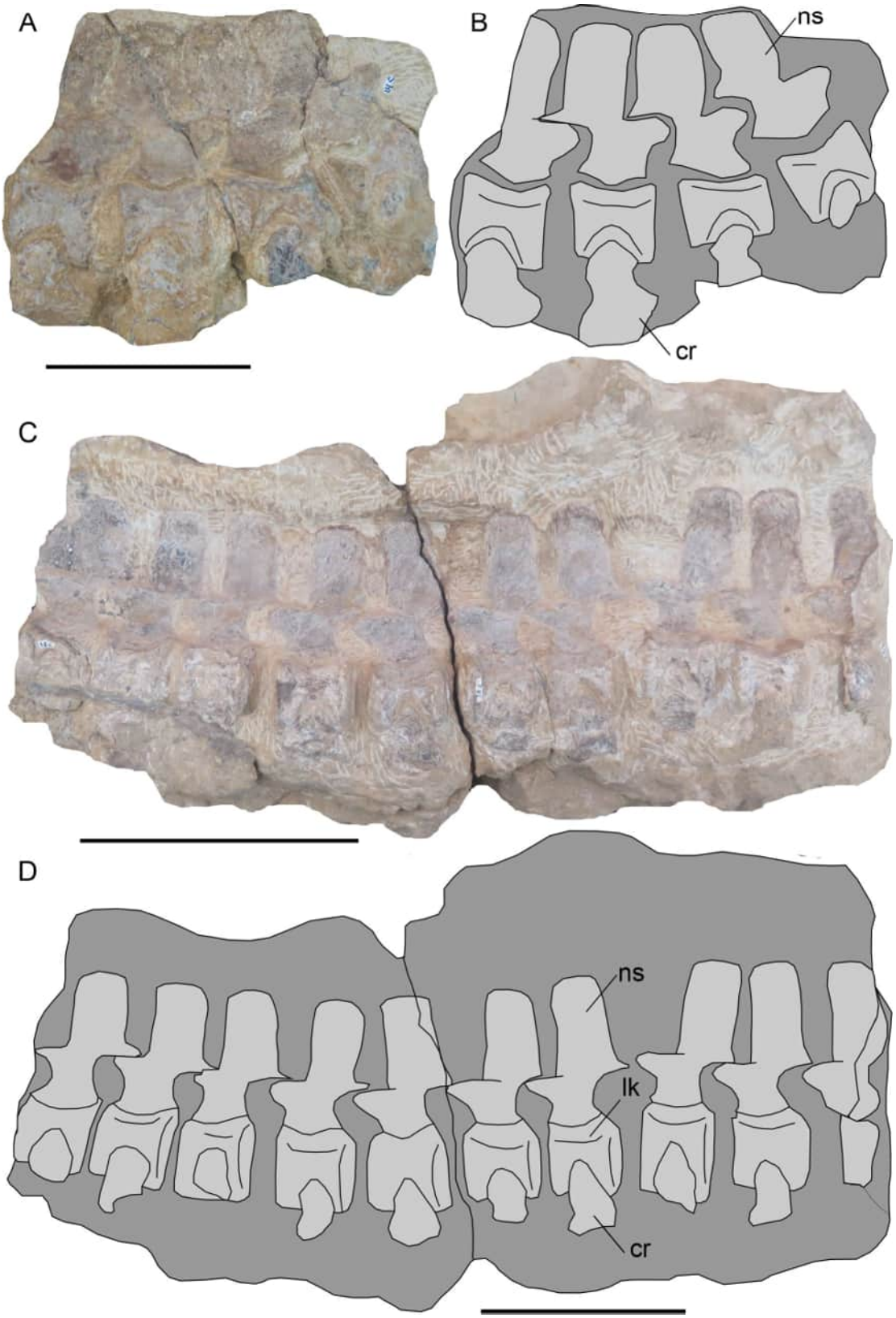

FIGURE 12. *Tuarangisaurus keyesi* (MPEF-PV 12001). Cervical vertebrae. **A-B** anterior middle cervical vertebrae in right lateral view, **A**, photo, **B**, diagram; **C-D** posterior middle in left lateral view, **C**, photo, **D**, diagram. Scale bar equals 100 mm

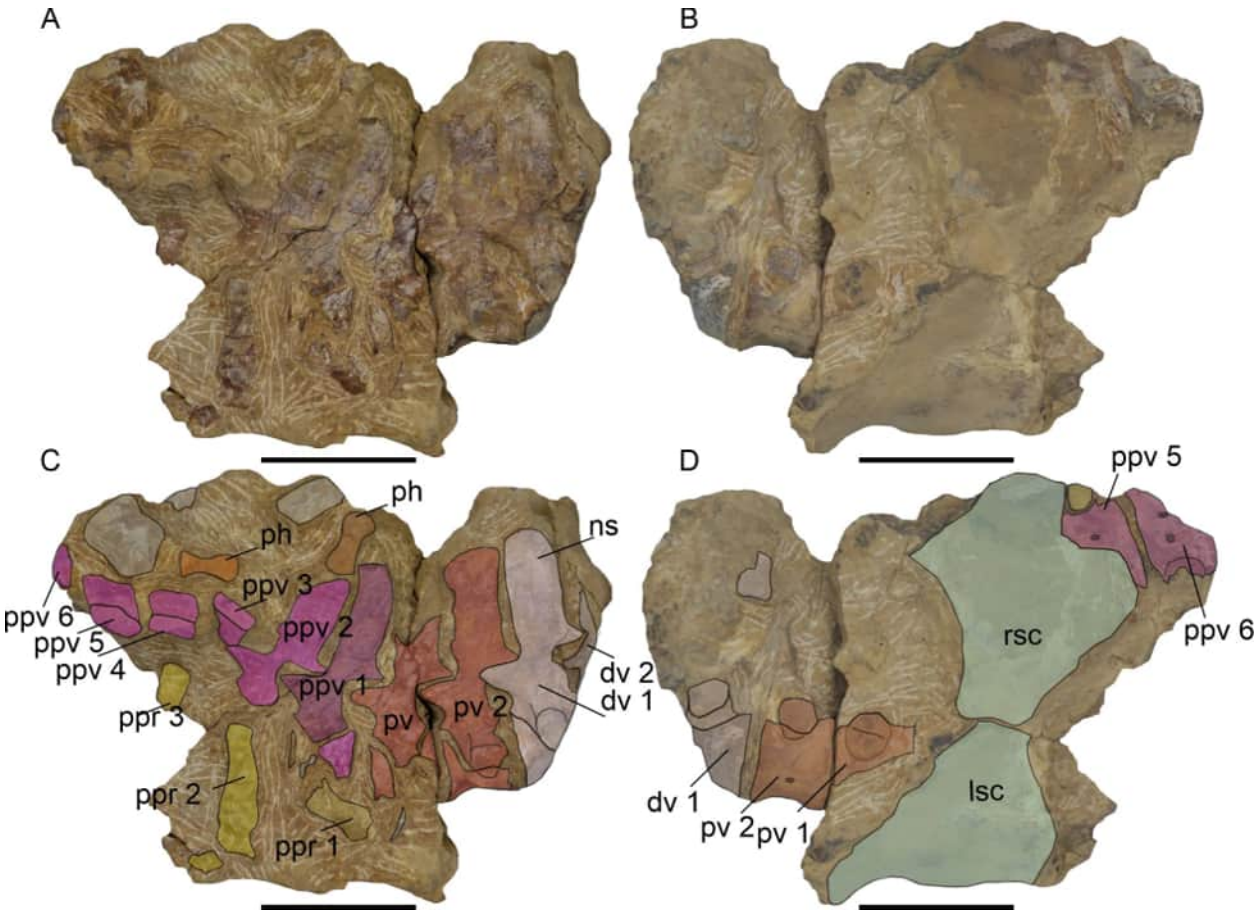

FIGURE 13. *Tuarangisaurus keyesi* (MPEF-PV 12001). Posteriormost cervicals, pectorals and anteriormost dorsal vertebrae, ribs and phalanges and scapulae natural moulds, **A**, **B**, photos and **C**, **D**, diagram showing elements preserved. Scale bar equals 100 mm.

long and high. The lateral surface is anteroposteriorly concave. The ventral surface is pierced by two-thirds foramina. The neural arch shows long, laterally expanded diapophyses that are oriented laterally and slightly caudally. The distal ends expand craniocaudally and dorsally. The shaft of each diapophysis bears a small step on its anterior and ventral margins.

Ribs. All ribs are single headed. The anterior and middle cervical ribs are ventro-laterally directed and show a slightly expanded end (Figure 11F) while the posterior cervical ribs are straight and lack the symmetrical expansion (Figures 12A, C; 14B).

Posterio cervical and pectoral ribs are longer and with a caudally twisted distal end (Figure 15B). There are +7 dorsal curved ribs, single-headed with slightly concave tubercle. The cross-section changes from proximally circular to a distal flattened section.

Appendicular Skeleton

Pectoral girdle. The scapulae are not preserved, but the natural mould of their ventral plate clearly show a short symphysis in the middle line.

Anterior limb. The anterior limb is well preserved and articulated. The humerus preserves only its distal end that is rounded (Figure 16A). Both radius (75 mm wide/58 mm length) and ulna (55 mm wide/54 mm length) are wider than long. The radial facet of intermedium is small compared with the ulnar facet. Between radius and ulna there is an epipodial foramen. There is a rounded accessory element between ulna and ulnare identified as the pisiform. The phalanges are short and wide. The fifth metacarpal is fully shifted to the carpal row.

Gastroliths

There are at least 66 gastroliths. All are rounded polished stones. The gastroliths are not in the natural position as they are located lateral to the ribs (Figures 14A, C; 15A). Their size ranges

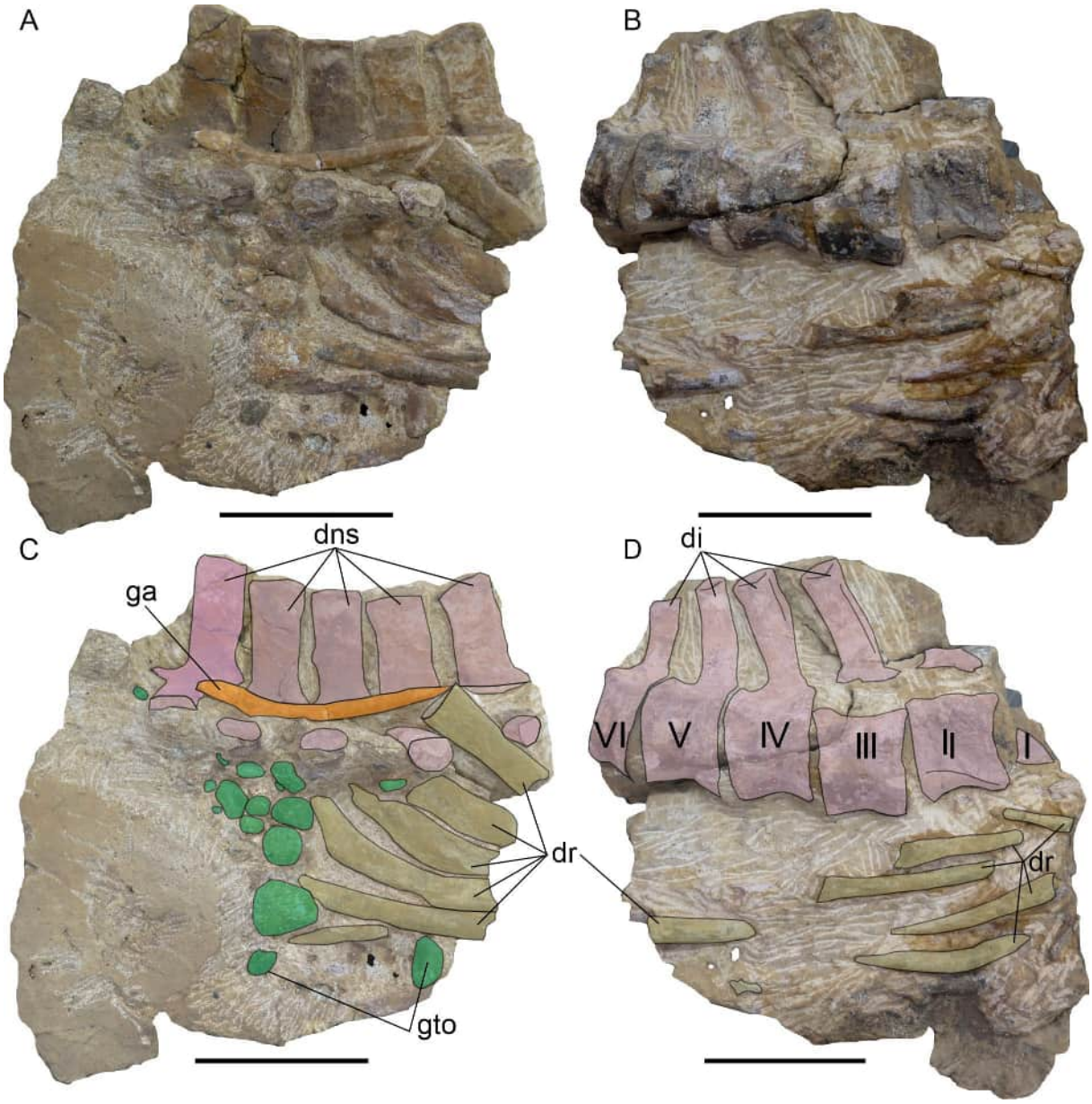

FIGURE 14. *Tuarangisaurus keyesi* (MPEF-PV 12001). Dorsal vertebrae, ribs and gastroliths, A, B, photos and C, D, diagram showing the preserved elements Scale bar equals 100 mm.

from 3 mm (long axis) to 40 mm in maximum length, with the largest clast measuring 32 mm along its intermediate axis.

PHYLOGENETIC RESULTS

The initial analysis recovered 18 MPTs of 1951 steps recovering (MPEF-PV 12001) as a sister group of *T. keyesi* (NPC CD 425 and NPC CD 426). The following TBR of the resulting trees recovered +20,000 trees but not shorter in terms of steps. The clade that comprises (MPEF-PV 12001) and (NPC CD 425 and NPC CD 426) is supported by Ch. 33.1 (participation of frontal in orbital margin); 109.3 (ectopterygoid strong posterior process posteroventrally directed) and 144.0 (hypapophysis low and round). Where both were scored as a single OTU the results are similar (+20,000 trees with 1951 steps). The general results are like those obtained by O'Gorman et al., (2024) and are therefore not discussed here (Figure 17).

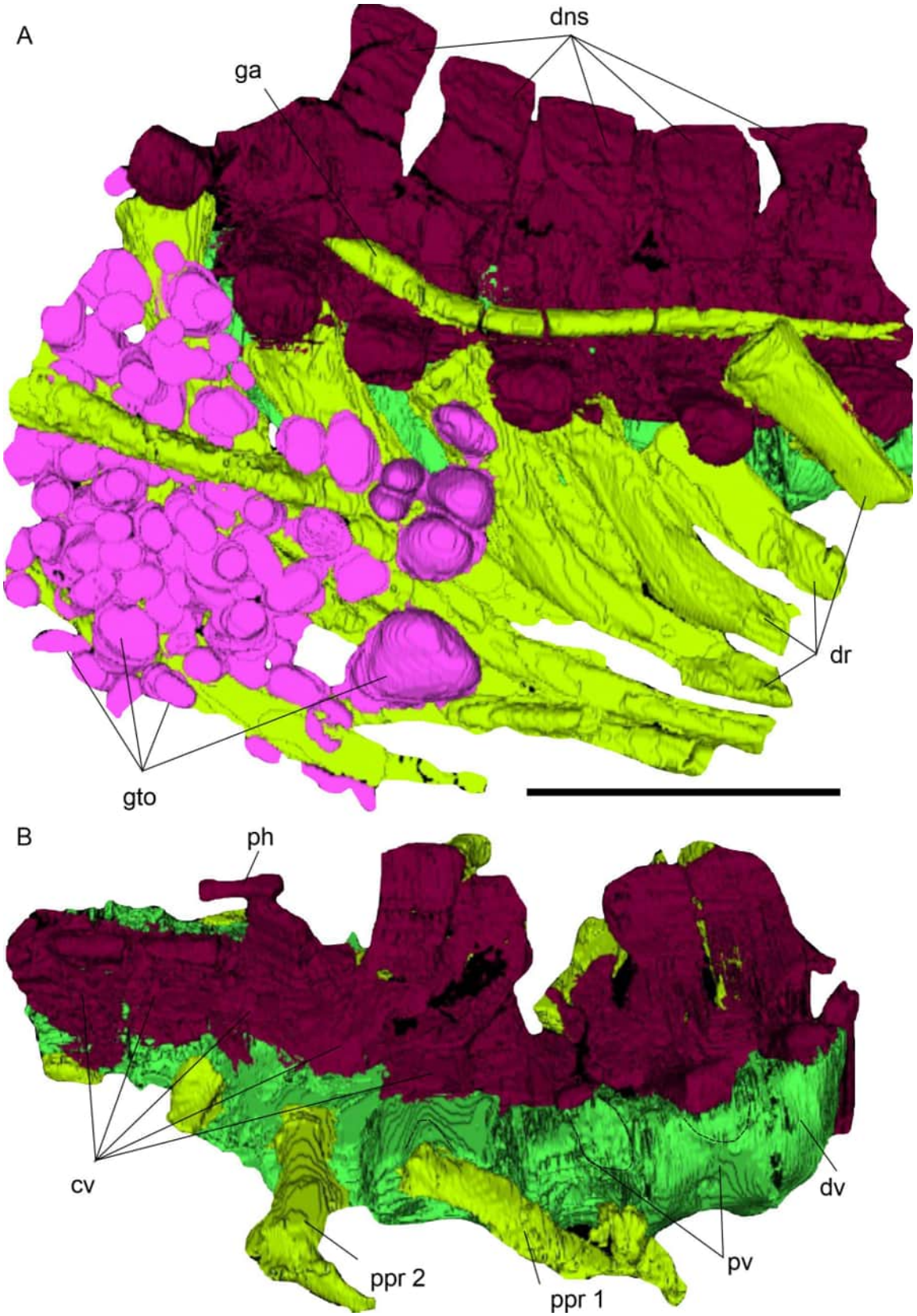

FIGURE 15. *Tuarangisaurus keyesi* (MPEF-PV 12001). **A-B,** 3D Segmentation. **A,** posteriormost cervicals, pectorals and first dorsal vertebrae in left lateral view, **B,** segment of dorsal region. Scale bar equals 100 mm.

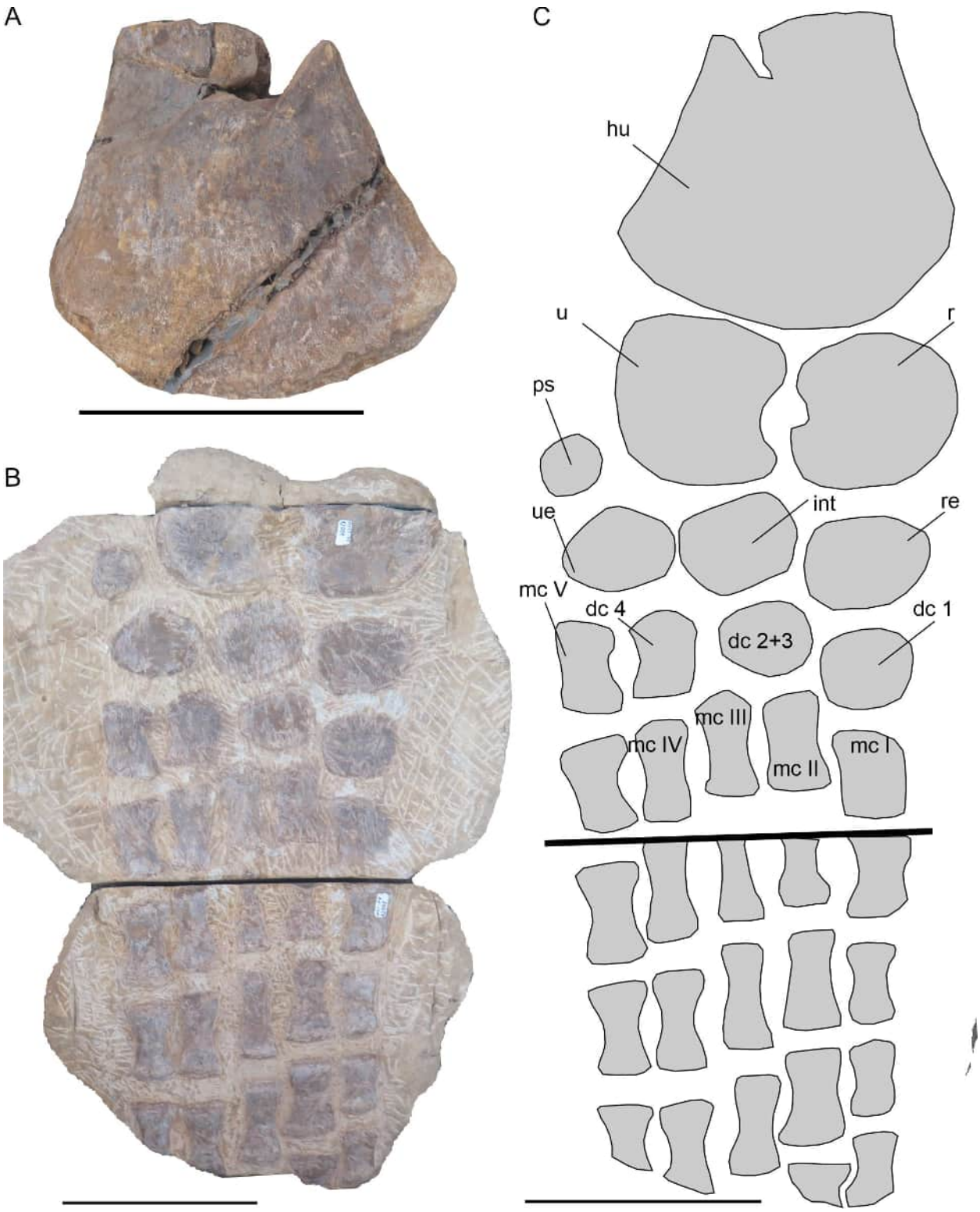

FIGURE 16. *Tuarangisaurus keyesi* (MPEF-PV 12001). **A-C,** Anterior limb. **A,** humerus distal end, **B**, epipodial, basipodial metapodial and phalanges, **C**, diagram showing preserved elements. Scale bar equals 100 mm.

TABLE 2. *Tuarangisaurus keyesi* (MPEF-PV 12001). Measurements of vertebral centra. L, length; H, height and B, breadth (all in mm), indexes HI, height (H)/length (L) ratio (HI = 100*H/L), BI, breadth (B)/length (L) ratio (BI = 100*B/L), BHI, breadth/height ratio (BHI = 100*B/H) and VLI, Vertebral Length Index [VLI = 100*L/(0.5*(H + B))]. Values in italics are approximated. c, cervical, d, dorsal, p, pectoral, pp, prepectoral, mc, middle cervical.

Position	L	H	B	HI	BI	BHI	VLI
1+2	31	13	22.1	42	71	-	-
3c	16	14	24	88	150	171	84
4c	18	-	-	-	-	-	-
5c	19	14	25	74	132	179	97
6c	19	15	25	79	132	167	95
7c	24	15	28	63	117	187	112
8c	22	-	29	-	132	-	-
9c	26	17	30	65	115	176	-
10c	25	-	29	-	116	-	-
11c	25	21	32	84	128	152	94
12c	25	-	38	-	152	-	-
13c	25	20	36	80	144	180	89
14c	24	-	-	-	-	-	-
15c	24	-	-	-	-	-	-
16c	26	-	-	-	-	-	-
17c	27	23	39	85	144	170	87
18c	30	-	-	-	-	-	-
19c	31	29	40	94	129	138	90
20c	32	-	40	-	125	-	-
21c	30	-	-	-	-	-	-
22c	30	-	-	-	-	-	-
23c	34	-	-	-	-	-	-
24c	31	-	-	-	-	-	-
25c	29	25	38	86	131	152	92
26c	31	-	-	-	-	-	-
27c	33	-	47	-	142	-	-
28c	31	-	-	-	-	-	-

DISCUSSION

Growth Stage and Systematic Affinities

The (MPEF-PV 12001) shows neural arches not fused to vertebral centrum in any vertebrae corresponding to the “juvenile” growth stage sensu Brown (1981) or osteologically mature individual sensu Araújo et al. (2015). Other features as the absence of fusion of the cervical ribs with vertebral centrum, rounded elements on the anterior limbs are consistent with this growth stage. The suture between neural arches and centra is V shaped. The shape of neurocentral suture has been indicated as a character that shows variance through ontogeny. Particularly neurocentral suture is U-shaped and V-shaped in adult and juvenile specimens of *Plesiosaurus*, respectively (Storrs, 1997). The presence of dumbbell shaped articular faces of cervical centra indicates Euelasmosaurida affinities (O’Gorman, 2019).

Affinities with *Tuarangisaurus keyesi*

The reexamination of the CT scan of the holotype of *Tuarangisaurus keyesi* (NPC CD 425), previously analyzed by O’Gorman et al. (2017), reveals that the skull is strongly compressed, causing distortion in the positions of the ectopterygoids. Both ectopterygoid are slightly displaced, and the caudal process was probably displaced and from its natural position attached to the lateral margin of the pterygoids and not as a separate process. Despite the length of this process, reaching the

TABLE 2 (continued).

Position	L	H	B	HI	BI	BHI	VLI
29c	31	-	-	-	-	-	-
30c	32	-	51	-	159	-	-
31c	35	-	-	-	-	-	-
32c	35	-	50	-	143	-	-
33c	36	36	50	100	139	139	84
34c	36	-	-	-	-	-	-
35c	40	-	-	-	-	-	-
36c	38	39	-	103	-	-	-
37c	-	-	-	-	-	-	-
38c	40	-	-	-	-	-	-
39c	40	-	-	-	-	-	-
mc3	39	39	60	100	154	154	79
mc1	36	38	64	106	178	168	71
mc2	36	39	64	108	178	164	70
pp5	37	39	73	105	197	187	66
pp4	38	37	72	97	189	195	70
pp3	37	-	73	-	197	-	-
pp2	37	-	73	-	197	-	-
pp1	39	46	74	118	190	161	65
p1	42	-	-	-	-	-	-
p2	44	50	77	114	175	154	69
d1	44	50	73	114	166	146	72
dn	49	46	-	94	-	-	-
dn+1	48	56	-	117	-	-	-
dn+2	47	53	50	113	106	94	91
dn+3	47	47	60	100	128	128	88
dn+4	46	49	59	107	128	120	85

middle level of the posterior interpterygoid vacuity and its position in a different plane from the body of the ectopterygoid is an autapomorphy of *Tuarangisaurus keyesi.* With this consideration the features observed in MPEF-PV 12001 support its assignment to *Tuarangisaurus keyesi* by the presence of ectopterygoid with ventral boss strongly projecting caudally and in a plane ventral to the ectopterygoid body (Ch. 109.3). However, there are some differences between MPEF-PV 12001 (osteologically immature) and the available material of *Tuarangisaurus keyesi* (NPC CD 425 and NPC CD 426, osteologically mature), see below. The main explanation of these differences is the difference in growth stage. The only well-preserved specimen of *Tuarangisaurus keyesi* with skull (NPC CD 425) is 370 mm in length, markedly larger than the skull of MPEF-PV 12001 (approximately 180 mm), generating a ratio 1 to 2. Additionally, the atlas-axis complex NPC CD 426 is 55 mm in length, whereas MPEF-PV 12001 shows a 31mm in length atlas-axis, generating a ratio of 1 to 1.8.

The ratio 1 to 2 or 1.8 is clearly explained by the difference in growth stage of (MPEF-PV 12001). This difference could also explain some differences between the holotype (NPC CD 425), referred specimen (NPC CD 426), and the specimen described here (MPEF-PV 12001) as all are related with the increases in skull relative height: 1] the subtle change in angle of the posterior embayment between the posterior margin of the squamosals symphysis in dorsal view, 2] the proportions of the basisphenoid is relatively lower and wider than the one of the NPC CD 425, and 3] the changes in the proportions of vertebrae are also related with the growth stage as the increases of the relative

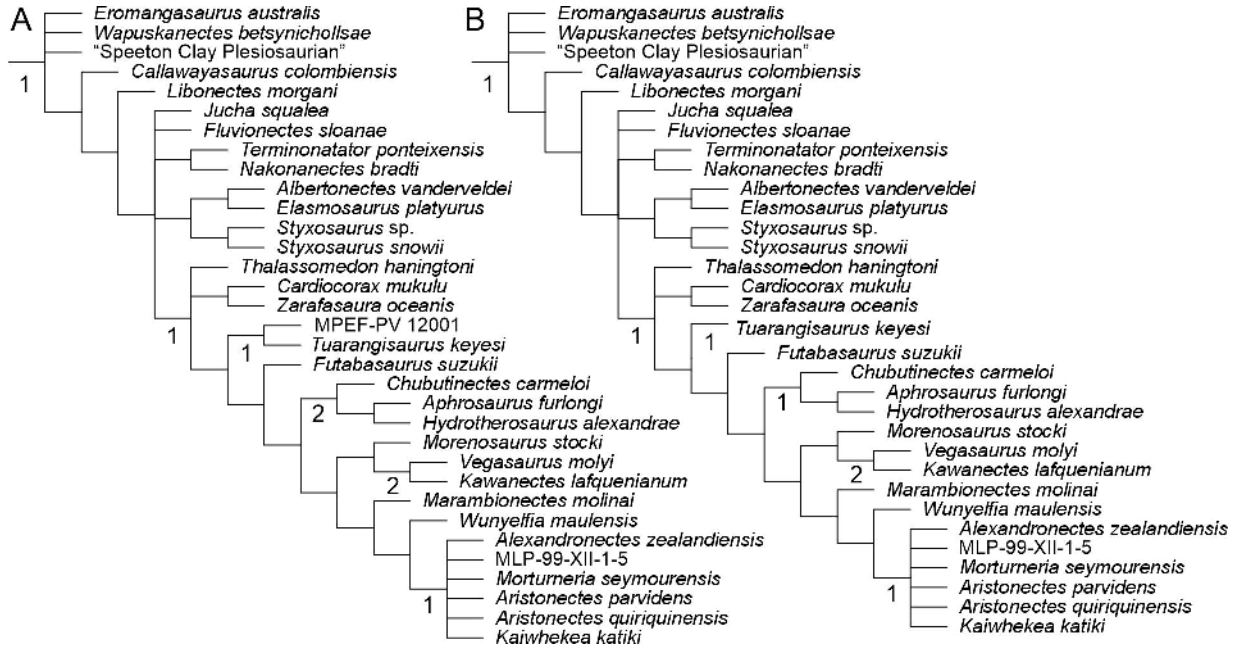

FIGURE 17. Consensus of the phylogenetic analysis. **A.** (1951 steps) considering the MPEF-PV 12001 and (CD 425 + CD 426) as a separate OTU. **B.** (1951 steps) considering (MPEF-PV 12001, referred material) and (CD 425 and CD 426, holotype) combined. Bremer supports below some nodes.

length of cervical during ontogeny is a feature previously observed in other elasmosaurids (O'Keefe and Hiller, 2006). The only differences observed not directly related with elongation are the process of the epipterygoid and the alveoli number. The presence of an anterior process of the epipterygoid observed in MPEF-PV 12001 (Figures 6A, D; 7A), not reconstructed in the holotype (O'Gorman et al., 2017: fig. 9H, I) could be explained by a poor preservation in this area in holotype (J.P. O'Gorman, personal obs). Whereas the differences in dentary alveoli number (2 alveoli) can be due intraspecific variation or difficult to evaluate the real number of alveoli as they tend to be confluent toward the posterior part of the mandible. An additional specimen of *T. keyesi,* NPC CD 427, is available; however, its extreme immaturity prevents a taxonomically meaningful direct comparison, except for the presence of the ectopterygoid posteroventral process (Otero et al., 2018). It also shares several general features, including the convex ventral margin of the orbit, the number of maxillary alveoli (14 in NPC CD 427 vs. ~16 in NPC CD 425 and MPEF-PV 12001), and the absence of the posterior interpterygoid symphysis (NPC CD 427 and MPEF-PV 12001).

COMPARISON OF MPEF-PV 12001 WITH OTHER ELASMOSAURIDS

The main features of MPEF-PV 12001 are discussed as well as the differences with other elasmosaurids.

Maxilla. The maxilla of MPEF-PV 12001 does not show a marked lateral expansion from the premaxilla, differing from *Callawayasaurus colombiensis, Libonectes morgani,* and *Cardiocorax mukulu* (Welles, 1962; Carpenter, 1997; Serratos et al., 2017; Marx et al., 2021). The maxilla forming a convex ventral margin of orbit is a common feature among elasmosaurids (O'Gorman, 2019) but absent in *Zarafasaura oceanis* and *Futabasaurus suzukii* (Vincent et al., 2011; Sato et al., 2006). The number of maxillary alveoli (16) is similar to other elasmosaurids except for *Zarafasaura oceanis* (13) and the aristonectines (Table 3).

Squamosal. MPEF-PV 12001 shows a posterior middle sized V-shaped notch on the posterior margin of the squamosal arch in dorsal view (inferred based in the position of supraoccipital) as in most elasmosaurids (Welles, 1962; Carpenter, 1999; Serratos et al., 2017; O'Gorman, 2019;) but differs from almost straight posterior margin of the CM Zfr 115 from New Zealand (referred to *Tuarangisaurus* sp.), *Callawayasaurus colombiensis, Eromangasaurus australis* and *Thalassomedon haningtoni* (Welles, 1943, 1962; Kear, 2007; Hiller et al., 2017;

TABLE 3. Maxillary and dentary alveoli among elasmosaurid.

Taxon	Maxillary / Dentary alveoli	Citation
Eromangasaurus australis	15–16? / 18	Kear, 2007
Callawayasaurus colombiensis	8+ / 19–20?	Welles, 1962
Libonectes morgani	14 / 18	Carpenter, 1999; pers. obs.
Terminonator ponteixensis	13+ / 17–18	Sato, 2003
Nakonanectes bradti	14 / 18–19	Serratos et al., 2017
Styxosaurus snowii	17 / ?	J.P.O'G pers. obs.
Cardiocorax mukulu	17 / 20	Marx et al., 2021
Zarafasaura oceanis	~13 / 15–16	Vincent et al., 2011; Lomax and Wahl, 2013
Thalassomedon haningtoni	11+ / 17	J.P.O'G pers. obs.
Tuarangisaurus keyesi	~16 / 21	O'Gorman et al., 2017
Futabasaurus suzukii	<15 / 20+	Sato et al., 2006
Morturneria seymourensis	38+ / ?	Chatterjee and Small, 1989
Aristonectes parvidens	51 / 63–65	Gasparini et al., 2003
Kaiwhekea katiki	36+ / 42–44	Cruickshank and Fordyce, 2002

J.P. O'Gorman Pers. Obs.); and the deep V shaped notch recorded in *Zarafasaura oceanis* and *Cardiocorax mukulu* and among the aristonectines (*Aristonectes quiriquinensis; Morturneria seymourensis, Kaiwhekea katiki* and *Alexandronectes zealandiensis* (Cruickshank and Fordyce, 2002; Lomax and Wahl, 2013; O'Keefe et al., 2017; Otero et al., 2018; O'Gorman et al., 2021; Marx et al., 2021).

Basioccipital. The occipital condyle is not well delimited by a neck differing from *Callawayasaurus colombiensis, Cardiocorax mukulu, Libonectes morgani* and *Nakonanectes bradti* (Welles, 1962; Allemand et al., 2017; Serratos et al., 2017; Marx et al., 2021, J.P. O'G. Pers Obs).

Parabasisphenoid. MPEF-PV 12001 shows a morphology not seen in any other elasmosaurid as the carotid artery enter the basisphenoid (only visible on the left side) laterally but there is not change from medio-lateral to antero-posterior direction of the carotid conduct prior to opening in the sella turcica. This differs from the observed in *Libonectes morgani, Tuarangisaurus keyesi,* and *Alexandronectes zealandiensis* (Allemand et al., 2017; O'Gorman et al., 2017; O'Gorman et al., 2021). It is possible that this difference be generated by the lack of complete ossification of the basisphenoid enclosing the carotid artery along a less extended length. Regarding the proportions of the. sella turcica it is significantly shorter and more open V shaped in dorsal view than the one described for *Libonectes morgani* (Allemand et al., 2017) and an indeterminate elasmosaurid from Russia (Zverkov et al., 2017) that are longer and U-shaped in dorsal view. The sella turcica of MPEF-PV 12001 is only slightly shorter and wider than the holotype of *Tuarangisaurus keyesi* (O'Gorman et al., 2017), but is it similar to the sella turcica of a juvenile elasmosaurids (MLP 15-I-7-6) from Vega Island (O'Gorman et al. 2018: fig. 3b) and *Aristonectes quiriquinensis* (O'Gorman et al., 2018; Otero et al., 2018). The differences with the holotype of *Tuarangisaurus keyesi* could be interpreted as ontogenetic variation. Additionally, the presence of similar proportions in *A. quiriquinensis* could be related with the retention of juvenile features, a condition previous proposed for aristonectines (O'Gorman et al., 2015). Additionally, the foramen from the VI cranial nerve is larger compared to the one recorded in the holotype of *T. keyesi* (O'Gorman et al, 2017:fig. 9E), similar to the foramen recoded in the specimen referred to *Libonectes morgani* (Allemand et al., 2017: Figure 5c, SMNS 81783) but smaller than the one of the holotype of *Libonectes morgani* (Serratos et al., 2017:sf5B, SMUSMP 69120). The ventral surface of the parabasisphenoid is formed by the parasphenoid that shows a well-marked keel as in other elasmosaurids with the exception of *Zarafasaura oceanis* and *Alexandronectes zealandiensis* (Otero et al., 2016; O'Gorman, 2019; O'Gorman et al., 2021; J.P. O'Gorman, Pers Obs). Additionally, the caudal end of the parasphenoid of MPEF-PV 12001 shows two small lateral projections additionally to a medial one that bears the keel. The caudal area is not covered by a posterior pterygoid symphysis in *Callawayasaurus colombiensis, Libonectes morgani, Nakonanectes bradti,* and *Zarafasaura oceanis* (Welles, 1962;

Carpenter, 1997; Lomax and Wahl, 2013; Serratos et al., 2017).

Exoccipital-opisthotic. The paraoccipital process of MPEF-PV 12001 is long and slender, however it is shorter than the observed in *Aristonectines quiriquinensis* (Otero et al., 2014). It articulates with the squamosal and pterygoid as in *Alexandronectes zealandiensis* but differs from *Cardiocorax mukulu* where the paraoccipital process articulates with squamosal and quadrate (O'Gorman et al., 2021; Marx et al., 2021). The distal end is unexpanded differing from the slightly expanded end of *Callawayasaurus colombiensis,* the expanded end of *Libonectes morgani* and *Nakonanectes bradti* (Welles, 1962; Carpenter, 1997; Serratos et al., 2017) and the extremely expanded end of *Alexandronectes zealandiensis* and *Cardiocorax mukulu* (O'Gorman et al., 2021; Marx et al., 2021).

Pterygoid. The pterygoid of MPEF-PV 12001 is similar to the pterygoid recorded in other elasmosaurids, however some differences are observed. MPEF-PV 12001 shows the pterygoid overlapping the vomer, a similar relationship was recorded in the holotype of *T. keyesi* (O'Gorman et al., 2017: fig. 8b, f). However, this is probably presented in other elasmosaurids but the absence of CT analyses precludes its confirmation. MPEF-PV 12001 does not show a posterior interpterygoid symphysis differing from *Callawayasaurus colombiensis, Libonectes morgani,* or *Nakonanectes bradti* (Welles, 1962; Carpenter, 1997; Serratos et al., 2017). But this absence of posterior pterygoid symphysis is also observed in *A. quiriquinensis* and *Alexandronectes zealandiensis* and an indeterminate elasmosaurid from the Snow Hill Island (O'Gorman et al., 2018, MLP 15-I-7-6) and *Cardiocorax mukulu* (Marx et al., 2021; Otero et al., 2016, 2018). The quadrate ramus of the pterygoid is continuous with the plates that limit laterally the posterior interpterygoid vacuity showing a gradual inflexion as the lateral margin becomes ventral and the dorsal surface become medial. A similar condition is observed in *Alexandronectes zealandiensis* and *Aristonectes quiriquinensis* (Otero et al., 2018; O'Gorman et al., 2021), and a similar condition seems to be present in *Cardiocorax mukulu* although there are some taphonomic distortion in that case (Marx et al., 2021). On the other side in *Callawayasaurus colombiensis* and *Libonectes morgani* the lateral plate ends caudally in a step that generates a separation between the lateral plate and quadrate ramus of pterygoid (Welles, 1962: fig. 4; Carpenter, 1997:fig. 2).

Ectopterygoid. The ectopterygoid of *Tuarangisaurus keyesi* (holotype and referred specimen CD 427, see Otero et al., 2018) shows a caudally directed long pointed process that follow the lateral plate of pterygoid until the middle level of the posterior interpterygoid vacuity. The ectopterygoid morphology is particularly variable among elasmosaurids. *Callawayasaurus colombiensis* shows a small ectopterygoid without caudal process. *Libonectes morgani* shows a short posterior process and bears an extremely rugose surface (Carpenter, 1997: fig. 2d). *Nakonanectes bradti* exhibits a pointed boss formed by ectopterygoid and pterygoid and the pterygoid form the anterior margin of the subtemporal fenestra (Serratos et al., 2017: fig. 5). The ectopterygoid of *Cardiocorax mukulu* is pointed anteriorly and bears a thickened area on the medial margin of the posterior border. This thickening runs caudally and ends following the same direction as the lateral margin of the pterygoid, this is relatively short and does not generate a caudal process (Marx et al., 2021: fig. 6A). The ectopterygoid of *Alexandronectes zealandiensis* is rhombic, with anterior and posterior pointed ends and with a rugose boss (O'Gorman et al., 2021: fig. 3C). The other well-known ectopterygoid from an aristonectine is the one of *A. quiriquinensis* that is anteroposteriorly elongated and with a caudal end at the level of the posterior margin of the basisphenoid but without the ventral inflexion, a feature absent in other elasmosaurids (Otero et al., 2018).

Mandible

The coronoid process is high and triangular, similar to the recorded in the holotype of *Tuarangisaurus keyesi* (although it is less gracile and less pointed (O'Gorman et al., 2017: fig. 9J) other Campanian–Maastrichtian elasmosaurids show also a high and triangular coronoid process such as *T. ponteixensis* (Sato, 2003: fig. 5), *N. bradti* (Serratos et al., 2017). On the other hand, *C. colombiensis* and *A. parvidens* exhibit a low and dorsally rounded coronoid processes (Welles, 1962; O'Gorman, 2016b: fig. 3.5), while the coronoid processes of the specimens referred to *L. morgani* may be low (SMU SMP 69120, Welles, 1962; Carpenter, 1997: fig. 2A), or high and subtriangular (SMNS 81783, Allemand et al., 2017: fig. 6c, Allemand et al., 2017: fig. 5). The orientation of the retroarticular process is likewise variable among elasmosaurids, being straight linear anteroposteriorly directed in MPEF-PV 12001 and the holotype of *T. keyesi* (Wiffen and Moisley, 1986), *L. morgani* (Sachs and Kear, 2017), and *N. bradti* (Serratos et al., 2017)

versus strongly posterodorsally directed in the aristonectines *Aristonectes* spp and *Kaiwhekea katiki* (Cruickshank and Fordyce, 2002; Gasparini et al. 2003; Otero et al., 2014), as well as in non aristonectine taxa, such as *Z. oceanis, Thalassomedon haningtoni,* and *Styxosaurus snowii* (Welles, 1943; Carpenter, 1999; Vincent et al., 2011; Otero, 2016).

Vertebral Column

The atlantal cup shows anterior surface heart shaped (wider dorsally than ventrally) similar to *Vegasaurus molyi, Thalassomedon haningtoni, Libonectes morgani, Nakonanectes bradti,* and *Albertonectes vanderveldei* (Kubo et al., 2012; Sachs and Kear, 2014; O'Gorman et al., 2015; Serratos et al., 2017) differing from *Marambionectes molinai* and the aristonectines *Aristonectes parvidens*, and *Wunyelfia maulensis* (O'Gorman, 2016a; Otero et al., 2021; O'Gorman et al., 2024). The ventral surface of the atlas-axis complex of MPEF-PV 12001 shows a low and rounded ventral hypapophysis shared with *Aristonectes parvidens, Wunyelfia maulensis,* and *Marambionectes molinai* (O'Gorman, 2016a; Otero et al., 2021; O'Gorman et al., 2024) but differing from *Libonectes morgani; Thalassomedon haningtoni; Vegasaurus molyi, Nakonanectes bradti,* and *Albertonectes vanderveldei* (Kubo et al., 2012; Sachs and Kear, 2014; O'Gorman et al., 2015; O'Gorman, 2016; Serratos et al., 2017). The atlas rib is long, and the axis rib is plate like, similar to the holotype of *Tuarangisaurus keyesi* (O'Gorman et al., 2017).

Cervical centra with lateral ridge are a feature usual among elasmosaurids with the exception of *Aristonectes parvidens; Kaiwhekea katiki* and *Nakonanectes bradti* (Cruickshank and Fordyce, 2002; O'Gorman, 2016a; Serratos et al., 2017; O'Gorman, 2019). Articular surfaces with ventral notch giving the bilobated articular faces is usual among elasmosaurids with the exception of the "Speeton Clay Plesiosaur", *Callawayasaurus colombiensis, Jucha squalea, Zarafasaura oceanis,* and *Traskasaura sandrae* (Welles, 1962; Lomax and Wahl, 2013; Fischer et al., 2020; O'Keefe et al., 2025). The cervical centra are longer than high (although it is a juvenile and therefore the adult form will likely become longer (Brown, 1981; O'Keefe and Hiller, 2006), differs from the aristonectines, *Zarafasaura oceanis, Cardiocorax mukulu,* and *Nakonanectes bradti* (Cruickshank and Fordyce, 2002; Lomax and Wahl, 2013; Serratos et al., 2017; Otero et al., 2018; Marx et al., 2021). The posterior cervical shows a Breadth/Length index lower than 200 differing from the aristonectines (Cruickshank and Fordyce, 2002; O'Gorman, 2019).

The anterior neural spines of MPEF-PV 12001 are rounded similar to the ones of *Zarafasaura oceanis, Vegasaurus molyi,* and *Kawanectes lafquenianus* (O'Gorman et al., 2015; O'Gorman, 2016; J.P. O'Gorman, Pers Obs) differs from the straight and caudally inclined neural spines of *Callawayasaurus colombiensis* or a rectangular-shaped neural spines of *Styxosaurus* and *Albertonectes vanderveldei* (Kubo et al., 2012; Otero, 2016) it also differs from the neural spines of anterior cervical of *Thalassomedon haningtoni* where the neural spines project slightly beyond the postzygapophysis (Welles, 1943).

Posterior neural spines are caudally inclined. A feature only recorded in the "Speeton Clay Plesiosaur" and *Callawayasaurus colombiensis,* differing from other Weddellonectia such as *Futabasaurus suzukii, Aphrosaurus furlongi, Kawanectes lafquenianus,* or the aristonectine *Aristonectes quiriquinensis* where neural spines tend to be cranially inclined (Sato et al., 2006; O'Gorman, 2016b, 2019; Otero et al., 2014, 2018). MPEF-PV 12001 has two pectoral vertebrae, differing from *Vegasaurus molyi* (3) *Aphrosaurus furlongi* (3); *Hydrotherosaurus alexandrae* (3); and *Aristonectes quiriquinensis* (3) but it is similar to *Morenosaurus stocki* (2) (Welles, 1943; O'Gorman et al., 2015, 2019; Otero et al., 2018).

The radius and ulna are wider than long, differing from the elongated *Callawayasaurus colombiensis, Zarafasaura oceanis,* and *Aristonectes quiriquinensis* (Welles, 1962; Lomax and Wahl, 2013; Otero et al., 2014). The anterior limbs bear an accessory ossicle between the ulna and ulnare, feature shared with *Morenosaurus stocki; Nakonanectes bradti; Aphrosaurus furlongi; Futabasaurus suzukii; Kawanectes lafquenianus; Chubutinectes carmeloi* and the aristonectine *Aristonectes quiriquinensis* (Welles, 1943; Sato et al., 2006; O'Gorman, 2016b; Otero et al., 2014; Serratos et al., 2017; O'Gorman, 2019).

Gastroliths. The gastrolith cluster is not easy to analyze as it is covered by matrix. However, the approximate number assessed (66) is relatively low compared with other elasmosaurids (See O'Gorman et al., 2025 and references cited there). This low number could be related to taphonomic loss as part of the main gastrolith cluster is cut by the weathered surface and therefore some gastroliths were lost prior to collection.

Hyoid Apparatus Among Plesiosaurians

The hyoid apparatus or hyobranchial apparatus (McClearn and Noden, 1988) is formed in reptiles by an unpaired element, the basihial, and paired ceratobranchials (sensu Schumacher, 1973) and other, less constant elements such as the ceratohyal (Figure 18). The paired ceratobranchials are usually two pairs of elements called CB I (anterior) and CB II (posterior) that articulate laterally to the *corpus hyoidei* (Li and Clarke, 2015). Among turtles the hyoid apparatus was detailed reviewed by (Jorgewich-Cohen et al., 2024). The hyoid apparatus of turtles shows a median anterior process, ceratobranchials I and ceratobranchials II. The level of ossification is variable, but the most frequent condition is the presence of fully ossified ceratobranchials I and ceratobranchials II (Jorgewich-Cohen et al., 2024 and references therein, Figure 18A). Among sphenodonts (Figure 18B) shows a basihial and seven elements articulated. Anteriorly, there are three anterior cartilaginous projections (a middle entoglossal process and a pair of hypohyals anterior processes). Caudally there are the ceratobranchials I (CB I), the only elements to be consistently ossified and the ceratobranchials II (CB II) that are cartilaginous extensions of the basihial that project caudally (Font and Rome, 1990; Schwenk, 1986; Tanner and Avery, 1982). Among squamata there is a wide variation in hyoid apparatus morphology that generates some problems related to homology of the elements, modifications of the basic model (Figure 18C). However regarding the, cornua, it is a consensus that, when only one pair is present, it is homologous to the anterior one (CB I) because 1] it retain the position (laterally) and articulate cranially and medially with other elements; 2] the ossified

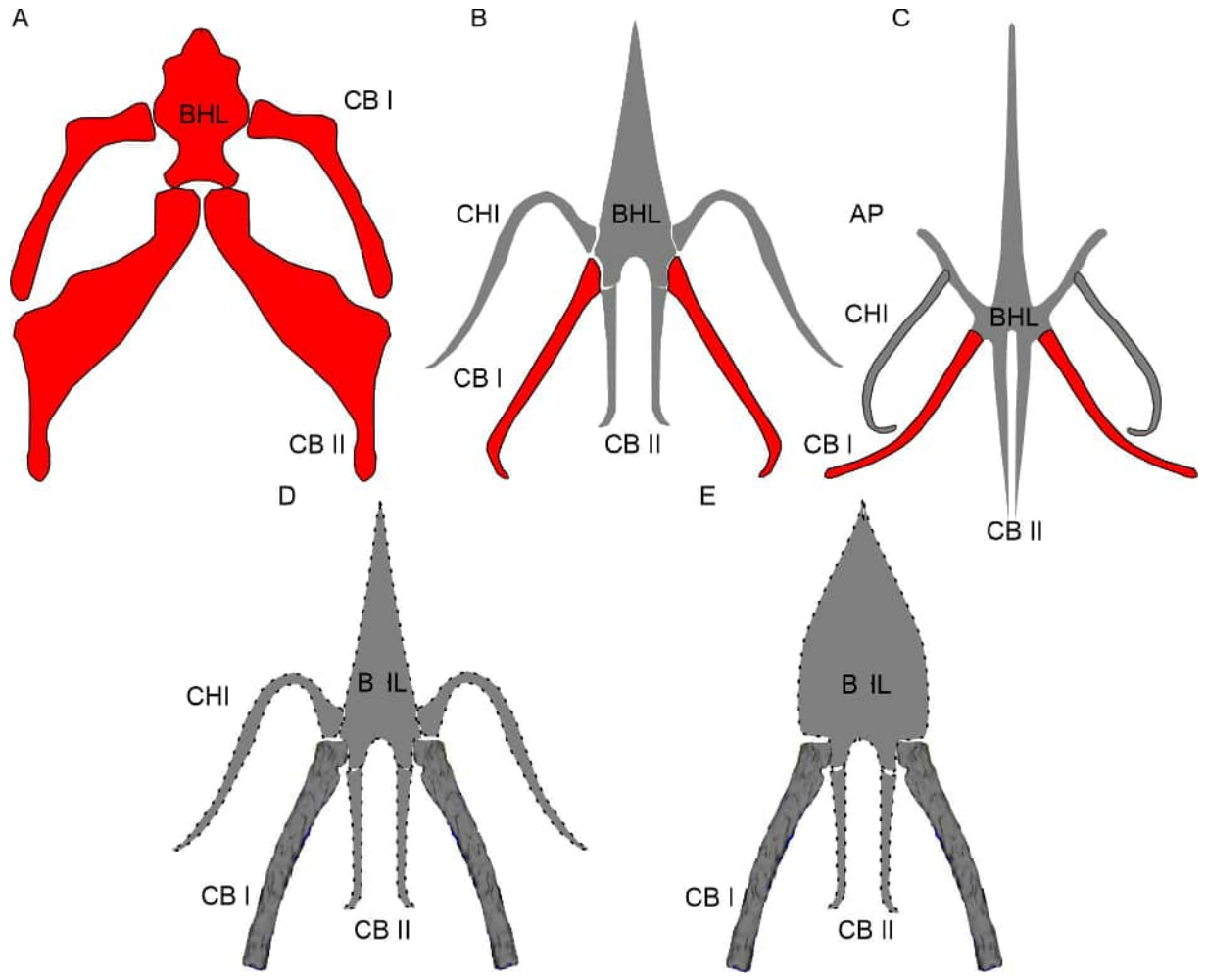

FIGURE 18. Hyoid apparatus of reptiles. **A-C,** extant species. **A**, Turtles (*Pelochelys cantorii*, redrawn from Jorgewich-Cohen et al., 2024); **B**, Sphenodontid (*Sphenodon punctatus* redrawn from Jones et al., 2009); **C,** Agamid squamate (*Pogona muricatus* redrawn from Schwenk, 2000), **D**, **E**, possible reconstructions of *T. keyesi.*

condition; 3] the present of a synovial joint to the basihial; 4] it serves as the insertion for the hyoglossus muscles (Langebartel, 1968; Schwenk, 2000); and 5] the tendency to reduce and lose posterior visceral arch elements first (Langebartel, 1968; Schwenk, 2000). Considering the previous general background, a possible reconstruction of the hyobranchial apparatus of MPEF-PV 12001 are given in Figure 18D, E based on the one of *Sphenodon punctatus.* With the presence of divided proximal end of the CB I allow the inference of a process of basihial with or without an associated ceratohyal (Figure 18D, E).

The presence of ossified hyoid apparatus is common among Sauropterygia (Table 4), although it is unknown in some species because of poor preservation. Among Placodontia, *Cyamodus orientalis* shows two pairs of ossified elements identified as ceratobranchials (Wang et al., 2019). Among pachypleurosaurids *Luopingosaurus imparilis* (Xu et al., 2023)*, Neusticosaurus pusillus, Neusticosaurus peyeri* (Sander, 1989) and *Keichousaurus hui* (Holmes et al., 2008) the ossified hyoid apparatus is restricted to a single pair of elements. The same is observed in the pistosaurid *Yunguisaurus liae* (Cheng et al., 2006). In all cases they are interpreted here as ceratobranchials I. In *Keichousaurus hui* and *Yunguisaurus liae* ceratobranchials I are located in the posterior half of the palate and laterally to the pterygoids (Cheng et al., 2006; Holmes et al., 2008). Among plesiosaurians, ossified hyoid apparatus has been recorded in different families, although several specimens lack it, probably for poor preservation. Among the better preserved examples, it is the ones of *Meyerasaurus victor,* which is a rod-like bone that shows proximal expanded end that is divided in two orthogonal planes (Smith and Vincent, 2010: fig. 2D). This configuration is similar to the one recorded in *Tuarangisaurus keyesi.* However, other plesiosaurs such as *Trinacromerum bentonianum* show an expanded proximal end but no division in different planes is present (Williston, 1908). Therefore, the unpreserved portions of the hyoid apparatus of plesiosaurians probably show at least a little variation. However, it is worth of noting that where the CB I are preserved in almost natural position *(Meyerasaurus victor, Eromangasaurus australis,* MPEF-PV 12001) they are placed near the posterior part of the palate on both sides of the posterior interpterygoid vacuity.

The presence of a gracile stick-like CB I among plesiosaurians is relevant as this morphology of the hyoid apparatus is correlated with the type of prey capture in terms of ram feeders vs suction feeders. Here 'ram feeders' refer to species that capture preys moving their body toward prey. On the other side "suction feeders" draw prey closer by suction before capture (Motani et al., 2013). Following the results of Motani et al. (2013) and Delsett et al. (2023) the morphology recorded among plesiosaurs is more consistent with ram feeders than with suction feeders, which usually shows longer and stockier hyobranchial apparatus.

Weddellian Province Elasmosaurid Fauna

The presence of *Tuarangisaurus keyesi* strengthens the relationship between the marine reptiles of the Weddellian Province (WP hereafter, Figure 19) previously assessing by other authors (Novas et al., 2002; Gasparini et al., 2003; O'Gorman et al., 2019, O'Gorman et al., 2015; Otero et al., 2018). This paleobiogeography connection is clearly represented in phylogenetic reconstruction by the clade Weddellonectia that comprises aristonectines and non aristonectine elasmosaurids. Aristonectine are distributed among the Weddellian Province with *Aristonectes parvidens* (Argentina, Gasparini et al., 2003); *Aristonectes quiriquinensis* (Chile, Otero et al., 2014); *Morturneria seymouren-*

TABLE 4. Sauropterygians with ossified hyoid apparatus have been recorded.

Taxon	Pairs	Citation
Borealonectes russelli	One pair	Sato and Wu, 2008
Meyerasaurus victor	One pair	Smith and Vincent, 2010
Peloneustes philarchus	One pair?	Ketchum and Benson, 2011
Edgarosaurus muddi	One pair	Druckenmiller, 2002
Polycotylus latipinnis	One pair	Schumacher and Martin, 2016
Trinacromerum bentonianum	One pair?	Williston, 1908
Eromangasaurus australis	One pair	Kear, 2007
Callawayasaurus colombiensis	One pair	Welles, 1962
Tuarangisaurus keyesi	One pair	O'Gorman et al., 2017

FIGURE 19. Weddellian Province (modified after Cruickshank and Fordyce, 2002).

sis (Antarctica, O'Keefe et al., 2017) and *Kaiwhekea katiki* (New Zealand, Cruickshank and Fordyce, 2002). Additionally, the non-aristonectine weddellonectians also show the same relationships with *Kawanectes lafquenianus* and *Chubutinectes carmeloi* (Patagonia, O'Gorman, 2016b; O'Gorman et al., 2023); *Marambionectes molinai* (Antarctica, O'Gorman et al., 2024) and *Tuarangisaurus keyesi* (New Zealand and Patagonia, Wiffen and Moisley, 1986). Additionally other non weddellian elasmosaurids are recovered within the weddellonectian such as *Aphrosaurus furlongi*, *Morenosaurus stocki, Hydrotherosaurus alexandrae,* (California, Welles, 1943 O'Gorman, 2019) and *Futabasaurus suzukii* (Japan Sato et al., 2006) and indeterminate aristonectines from Angola (Araújo et al., 2015). All this indicate the presence of a major clade that occupy the Weddellian Province extending thought the Atlantic to West Africa and on the other side to the north coasts of the pacific.

CONCLUSIONS

Tuarangisaurus keyesi represents the first and only non-aristonectine elasmosaurid recovered from the Lefipán Formation.

The basicranium basisphenoid in early ontogenetic stages of the non-aristonectines show similarities with the *Aristonectes*

The hyoid apparatus of *Tuarangisaurus keyesi* is similar to the record of other Plesiosauria and it is consistent with ram feeders.

ACKNOWLEDGEMENTS

This contribution was supported by PICT-2018-02443, PICT-2021-748 GRF-TII-00236 and National Geographic Society project NGS-92822R-22. The authors thanks P. Puerta (MPEF), A. Dajil, and S. Koefoed for providing help in field work. F. Sollary Orellana for part of the fossil preparation and the MPEF and MLP for allowing the fossil preparation in its labs. Lic. M.A. Tanuz, Dra. B. Aguirre Urreta (UBA) and E. Ruigomez (MPEF) for allowing the study of the materials under their care. The authors would like to thank Dr. S. Tartaglione and the operating technician Lic. C. Ríos (CIM, Centro de Imágenes Medicas, Trelew, Chubut, Argentina) and J. Muiño (Hospital San Martin, La Plata, Argentina) for collaborating with the CT scans. The authors thank T. Ybarra, the landowner of the field site. Finally, the authors thanks the Wlli Hennig Society for the TNT free software. Finally, we thank two anonymous reviewers for the comments that improved this contribution.

REFERENCES

Allemand, R., Bardet, N., Houssaye, A., and Vincent, P. 2017. Virtual reexamination of a plesiosaurian specimen (Reptilia, Plesiosauria) from the Late Cretaceous (Turonian) of Goulmima, Morocco, using computed tomography. Journal of Vertebrate Paleontology 37:e1325894. https://doi.org/10.1080/02724634.2017.1325894

Andrews, C.W. 1913. A descriptive catalogue of the marine reptiles of the Oxford Clay. Based on the Leeds Collection in British Museum (Natural History), Part II. British Museum (Natural History), London, 206 pp. https://doi.org/10.5962/bhl.title.61785

Araújo, R., Polcyn, M.J., Lindgren, J., Jacobs, L.L., Schulp, A.S., Mateus, O., Gonçalves, A.O., and Morais, M.-L. 2015. New aristonectine elasmosaurid plesiosaur specimens from the Early Maastrichtian of Angola and comments on paedomorphism in plesiosaurs. Netherlands Journal of Geosciences 94:93–108. https://doi.org/10.1017/njg.2014.43

Benson, R.B. and Druckenmiller, P.S. 2014. Faunal turnover of marine tetrapods during the Jurassic–Cretaceous transition. Biological Reviews 89:1–23. https://doi.org/10.1111/brv.12038

Brown, D.S. 1981. The English Upper Jurassic Plesiosauroidea (Reptilia) and a review of the phylogeny and classification of the Plesiosauria. Bulletin of the British Museum (Natural History), Geology Series 35:253–347.

Cabrera, A. 1941. Un plesiosaurio nuevo de Cretáceo del Chubut. Revista del Museo de La Plata (Nueva Serie) 2:113–130.

Carpenter, K. 1997. Comparative cranial anatomy of two North American Cretaceous plesiosaurs. In Callaway, J.M. and Nicholls, E.L. (eds.), Ancient Marine Reptiles. Academic Press, San Diego, p. 191–216. https://doi.org/10.1016/b978-012155210-7/50011-9

Carpenter, K. 1999. Revision of North American elasmosaurs from the Cretaceous of the Western Interior. Paludicola 2:148–173.

Casadio, S. 1998. Las ostras del límite Cretácico–Paleógeno de la cuenca Neuquina (Argentina). Su importancia bioestratigráfica y paleobiogeográfica. Ameghiniana 35:449–471.

Chatterjee, S. and Small, B.J. 1989. New plesiosaur from the Upper Cretaceous of Antarctica. Special Publications of the Geological Society 47:197–215.

Cope, E.D. 1869. Synopsis of the extinct Batrachia, Reptilia and Aves of North America. Transactions of the American Philosophical Society (new series) 14:1–252. https://doi.org/10.5962/bhl.title.60499

Cruickshank, A.R.I. and Fordyce, R.E. 2002. A new marine reptile (Sauropterygia) from New Zealand: further evidence for a Late Cretaceous austral radiation of cryptoclidid plesiosaurs. Palaeontology 45:557–575. https://doi.org/10.1111/1475-4983.00249

Cheng, Y.N., Sato, T., Wu, X.C., and Li, C. 2006. First complete pistosaurid from the Triassic of China. Journal of Vertebrate Paleontology 26:501–504. https://doi.org/10.1671/0272-4634(2006)26[501:fcpftt]2.0.co;2

de Blainville, H.D. 1835. Description de quelques espèces de reptiles de la Californie, précédée de l'analyse d'un système général d'herpétologie et d'amphibiologie. Nouvelles Archives du Museum d'Histoire Naturelle 4:233–296.

Delsett, L.L., Pyenson, N., Miedema, F., and Hammer, Ø. 2023. Is the hyoid a constraint on innovation? A study in convergence driving feeding in fish-shaped marine tetrapods. Paleobiology, 49:684–699. https://doi.org/10.1017/pab.2023.12

Druckenmiller, P.S. 2002. Osteology of a new plesiosaur from the Lower Cretaceous (Albian) Thermopolis Shale of Montana. Journal of Vertebrate Paleontology 22:29–42. https://doi.org/10.1671/0272-4634(2002)022[0029:ooanpf]2.0.co;2

Fazio, A.M., Liliana, N.C., and Scasso, R.A. 2013. Geoquímica de tierras raras y fosfogénesis en un engolfamiento marino del Cretácico Tardío–Paleoceno de Patagonia, Provincia del Chubut, Argentina. Revista Mexicana de Ciencias Geológicas 30:582–600.

Fischer, V., Benson, R.B., Druckenmiller, P.S., Ketchum, H.F., and Bardet, N. 2018. The evolutionary history of polycotylid plesiosaurians. Royal Society Open Science 5:172177. https://doi.org/10.1098/rsos.172177

Fischer, V., Zverkov, N.G., Arkhangelsky, M.S., Stenshin, I.M., Blagovetshensky, I.V., and Uspensky, G.N. 2020. A new elasmosaurid plesiosaurian from the Early Cretaceous of Russia marks an early attempt at neck elongation. Zoological Journal of the Linnean Society 192:1167–1194. https://doi.org/10.1093/zoolinnean/zlaa103

Font, E. and Rome, L.C. 1990. Functional morphology of dewlap extension in the lizard *Anolis equestris* (Iguanidae). Journal of Morphology 206:245–258. https://doi.org/10.1002/jmor.1052060210

Gasparini, Z., Bardet, N., Martin, J.E., and Fernández, M. 2003. The elasmosaurid plesiosaur *Aristonectes* Cabrera from the latest Cretaceous of South America and Antarctica. Journal of Vertebrate Paleontology 23:104–115. https://doi.org/10.1671/0272-4634(2003)23[104:tepacf]2.0.co;2

Hiller, N., O'Gorman, J.P., Otero, R.A., Mannering, A.A. 2017. A reappraisal of the Late Cretaceous Weddellian plesiosaur genus Mauisaurus Hector, 1874. New Zealand Journal of Geology and Geophysics 60: 112–128. https://doi.org/10.1080/00288306.2017.1281317

Holmes, R., Cheng, Y.N., and Wu, X.C. 2008. New information on the skull of *Keichousaurus hui* (Reptilia: Sauropterygia) with comments on sauropterygian interrelationships. Journal of Vertebrate Paleontology 28:76–84. https://doi.org/10.1671/0272-4634(2008)28[76:niotso]2.0.co;2

Jones, M.E.H., Curtis, N., O'Higgins, P., Fagan, M., and Evans, S.E. 2009. The head and neck muscles associated with feeding in *Sphenodon* (Reptilia: Lepidosauria: Rhynchocephalia). Palaeontologia Electronica 12(2):7A, 56 pp.

Jorgewich-Cohen, G., Werneburg, I., Jobbins, M., Ferreira, G.S., Taylor, M.D., Bastiaans, D., and Sánchez-Villagra, M.R. 2024. Morphological diversity of turtle hyoid apparatus is linked to feeding behavior. Integrative Organismal Biology 6:oba014. https://doi.org/10.1093/iob/obae014

Kear, B.P. 2007. Taxonomic clarification of the Australian elasmosaurid genus *Eromangasaurus*, with reference to other austral elasmosaur taxa. Journal of Vertebrate Paleontology 27:241–246. https://doi.org/10.1671/0272-4634(2007)27[241:tcotae]2.0.co;2

Ketchum, H.F. and Benson, R.B. 2011. The cranial anatomy and taxonomy of *Peloneustes philarchus* (Sauropterygia, Pliosauridae) from the Peterborough Member (Callovian, Middle Jurassic) of the United Kingdom. Palaeontology 54:639–665. https://doi.org/10.1111/j.1475-4983.2011.01050.x

Kubo, T., Mitchell, M.T., and Henderson, D.M. 2012. *Albertonectes vanderveldei*, a new elasmosaur (Reptilia, Sauropterygia) from the Upper Cretaceous of Alberta. Journal of Vertebrate Paleontology 32:557–572. https://doi.org/10.1080/02724634.2012.658124

Langebartel, D.A. 1968. The hyoid and its associated muscles in snakes. Illinois Biological Monographs 38. University of Illinois Press, Urbana. https://doi.org/10.5962/bhl.title.50273

Lesta, P. and Ferello, R. 1972. Región extrandina del Chubut y norte de Santa Cruz. In: Leanza, A.F. (ed.), Geología Regional Argentina. Academia Nacional de Ciencias de Córdoba, Córdoba, p. 601–654.

Li, Z. and Clarke, J.A. 2015. New insight into the anatomy of the hyolingual apparatus of *Alligator mississippiensis* and implications for reconstructing feeding in extinct archosaurs. Journal of Anatomy 227:45–61. https://doi.org/10.1111/joa.12320

Lomax, D.R. and Wahl, W.R. 2013. A new specimen of the elasmosaurid plesiosaur *Zarafasaura oceanis* from the Upper Cretaceous (Maastrichtian) of Morocco. Paludicola 9:97–109.

Martins, T.A.C.P., Santa Bárbara, A., Silva, G.B., Faria, T.V., Cassaro, B., and Silva, J.V.L. 2007. InVesalius: three-dimensional medical reconstruction software. In Virtual and Rapid Manufacturing. CRC Press, p. 135–141.

Marx, M.P., Mateus, O., Polcyn, M.J., Schulp, A.S., Gonçalves, A.O., and Jacobs, L.L. 2021. The cranial anatomy and relationships of *Cardiocorax mukulu* (Plesiosauria: Elasmosauridae) from Bentiaba, Angola. PLOS One 16:e0255773. https://doi.org/10.1371/journal.pone.0255773

McClearn, D. and Noden, D.M. 1988. Ontogeny of architectural complexity in embryonic quail visceral arch muscles. American Journal of Anatomy 183:277–293. https://doi.org/10.1002/aja.1001830402

Medina, F.A., Malagnino, E.C., and Camacho, H.H. 1990. Bioestratigrafía del Cretácico Superior–Paleoceno marino de la Formación Lefipán, Barranca de los Perros, río Chubut, Chubut. In V Congreso Argentino de Paleontología y Bioestratigrafía. Universidad Nacional de Tucumán, p. 137–142.

Morgan, D.J., III and O'Keefe, F.R. 2019. The cranial osteology of two specimens of *Dolichorhynchops bonneri* (Plesiosauria, Polycotylidae) from the Campanian of South Dakota, and a cladistic analysis of the Polycotylidae. Cretaceous Research 96:149–171. https://doi.org/10.1016/j.cretres.2018.11.027

Motani, R., Ji, C., Tomita, T., Kelley, N., Maxwell, E., Jiang, D.Y., and Sander, P.M. 2013. Absence of suction feeding ichthyosaurs and its implications for Triassic mesopelagic paleoecology. PLOS One 8:e66075. https://doi.org/10.1371/journal.pone.0066075

Novas, F.E., Fernández, M.S., de Gasparini, Z.B., Lirio, J.M., Nuñez, H.J., and Puerta, P. 2002. *Lakumasaurus antarcticus*, n. gen. et sp., a new mosasaur (Reptilia, Squamata) from the Upper Cretaceous of Antarctica. Ameghiniana 29:245–249.

O'Gorman, J.P. 2012. The oldest elasmosaurs (Sauropterygia, Plesiosauria) from Antarctica, Santa Marta Formation (upper Coniacian? Santonian-upper Campanian) and Snow Hill Island Formation (upper Campanian-lower Maastrichtian), James Ross Island. Polar Research 31:1–10. https://doi.org/10.3402/polar.v31i0.11090

O'Gorman, J.P. 2016a. A small body sized non-aristonectine elasmosaurid (Sauropterygia, Plesiosauria) from the Late Cretaceous of Patagonia with comments on the relationships of the Patagonian and Antarctic elasmosaurids. Ameghiniana 53:245–268. https://doi.org/10.5710/amgh.29.11.2015.2928

O'Gorman, J.P. 2016b. New insights on the *Aristonectes parvidens* (Plesiosauria, Elasmosauridae) holotype: news on an old specimen. Ameghiniana 53:397–417. https://doi.org/10.5710/amgh.24.11.2015.2921

O'Gorman, J.P. 2019. Elasmosaurid phylogeny and paleobiogeography with a reappraisal of *Aphrosaurus furlongi* from the Maastrichtian of the Moreno Formation. Journal of Vertebrate Paleontology 39: e1692025. https://doi.org/10.1080/02724634.2019.1692025

O'Gorman, J.P., Salgado, L., Varela, J., and Parras, A. 2013. Elasmosaurs (Sauropterygia, Plesiosauria) from the La Colonia Formation (Campanian–Maastrichtian), Argentina. *Alcheringa* 37:259–267. https://doi.org/10.1080/03115518.2013.745250

O'Gorman, J.P., Aspromonte, F.R., and Matelo Mirco, G. 2025. First record of lithophagy in *Sulcusuchus erraini* (Plesiosauria; Polycotylidae) with comments on the taphonomic and collect bias in gastroliths. Historical Biology, 1–13.

O'Gorman, J.P., Salgado, L., Olivero, E., and Marenssi, S. 2015. *Vegasaurus molyi*, gen. et sp. nov. (Plesiosauria, Elasmosauridae), from the Cape Lamb Member (lower maastrichtian) of the Snow Hill Island Formation, Vega Island, Antarctica, and remarks on Wedellian Elasmosauridae. Journal of Vertebrate Paleontology e931285. https://doi.org/10.1080/02724634.2014.931285

O'Gorman, J.P., Otero, R.A., Hiller, N., Simes, J., and Terezow, M. 2017. Redescription of *Tuarangisaurus keyesi* (Sauropterygia; Elasmosauridae), a key species from the uppermost Cretaceous of the Weddellian Province: internal skull anatomy and phylogenetic position. Cretaceous Research 71:118–136. https://doi.org/10.1016/j.cretres.2016.11.014

O'Gorman, J.P., Coria, R.A., Reguero, M., Santillana, S., Mörs, T., and Cárdenas, M. 2018. The first non-aristonectine elasmosaurid (Sauropterygia; Plesiosauria) cranial material from Antarctica: new data on the evolution of the elasmosaurid basicranium and palate. Cretaceous Research 89:248–263. https://doi.org/10.1016/j.cretres.2018.03.013

O'Gorman, J.P., Santillana, S., Otero, R., and Reguero, M. 2019. A giant elasmosaurid (Sauropterygia; Plesiosauria) from Antarctica: new information on elasmosaurid body-size diversity and aristonectine evolutionary scenarios. Cretaceous Research 102:37–58. https://doi.org/10.1016/j.cretres.2019.05.004

O'Gorman, J.P., Otero, R.A., Hiller, N., O'Keefe, F.R., Scofield, R.P., and Fordyce, R.E. 2021. CT-scan description of *Alexandronectes zealandiensis* (Elasmosauridae, Aristonectinae), with comments on the elasmosaurid internal cranial features. Journal of Vertebrate Paleontology e1923310. https://doi.org/10.1080/02724634.2021.1923310

O'Gorman, J.P., Carignano, A.P., Calvo-Marcilese, L., and Panera, J.P.P. 2023. A new elasmosaurid (Sauropterygia, Plesiosauria) from the upper levels of the La Colonia Formation (upper Maastrichtian), Chubut Province, Argentina. Cretaceous Research 152:105674.
https://doi.org/10.1016/j.cretres.2023.105674

O'Gorman, J.P., Canale, J.I., Bona, P., Tineo, D.E., Reguero, M., and Cárdenas, M. 2024. A new elasmosaurid (Plesiosauria: Sauropterygia) from the López de Bertodano Formation: new data on the evolution of the aristonectine morphology. Journal of Systematic Palaeontology 22:2312302.
https://doi.org/10.1080/14772019.2024.2312302

O'Gorman, J.P., Aspromonte, F.R., and Matelo Mirco, G. 2025. First record of lithophagy in *Sulcusuchus erraini* (Plesiosauria; Polycotylidae) with comments on the taphonomic and collect bias in gastroliths. Historical Biology, 1–13.

O'Keefe, F. R., and Hiller, N. 2006. Morphologic and ontogenetic patterns in elasmosaur neck length, with comments on the taxonomic utility of neck length variables. Paludicola 5:206–229.

O'Keefe, F.R. and Street, H.P. 2009. Osteology of the cryptocleidoid plesiosaur *Tatenectes laramiensis*, with comments on the taxonomic status of the Cimoliasauridae. Journal of Vertebrate Paleontology 29:48–57.
https://doi.org/10.1671/039.029.0118

O'Keefe, F.R., Otero, R.A., Soto-Acuña, S., O'Gorman, J.P., Godfrey, S.J., and Chatterjee, S. 2017. Cranial anatomy of *Morturneria seymourensis* from Antarctica, and the evolution of filter feeding in plesiosaurs of the austral Late Cretaceous. Journal of Vertebrate Paleontology 37:e1347570.
https://doi.org/10.1080/02724634.2017.1347570

O'Keefe, F.R., Armour Smith, E., Clark, R.O., Otero, R.A., Perella, A., and Trask, P. 2025. A name for the Provincial Fossil of British Columbia: a strange new elasmosaur taxon from the Santonian of Vancouver Island. Journal of Systematic Palaeontology 23: 2489938.
https://doi.org/10.1080/14772019.2025.2489938

Olivero, E.B., Medina, F.A., and Camacho, H.H. 1990. Nuevos hallazgos de moluscos con afinidades australes en la Formación Lefipán (Cretácico superior, Chubut): significado paleogeográfico. In: V Congreso Argentino de Paleontología y Bioestratigrafía, Tucumán, Argentina, Actas 1:129–135.

Otero, R.A. 2016. Taxonomic reassessment of *Hydralmosaurus* as *Styxosaurus*: new insights on the elasmosaurid neck evolution throughout the Cretaceous. PeerJ 4:e1777.
https://doi.org/10.7717/peerj.1777

Otero, R.A., Soto-Acuña, S., and Rubilar-Rogers, D. 2012. A postcranial skeleton of an elasmosaurid plesiosaur from the Maastrichtian of central Chile, with comments on the affinities of Late Cretaceous plesiosauroids from the Weddellian Biogeographic Province. Cretaceous Research 37:89–99.
https://doi.org/10.1016/j.cretres.2012.03.010

Otero, R.A. and O'Gorman, J.P. 2013. Identification of the first postcranial skeleton of *Aristonectes* Cabrera (Plesiosauroidea, Elasmosauridae) from the upper Maastrichtian of the south-eastern Pacific, based on a bivariate graphic analysis. Cretaceous Research 41:86–89.
https://doi.org/10.1016/j.cretres.2012.11.001

Otero, R.A., Soto-Acuña, S., O'Keefe, F.R., O'Gorman, J.P., Stinnesbeck, W., Suárez, M.A., Rubilar-Rogers, D., Quinzio-Sinn, L.A., and Salazar, C. 2014. *Aristonectes quiriquinensis* sp. nov., a new highly derived elasmosaurid from the upper Maastrichtian of central Chile. Journal of Vertebrate Paleontology 34:100–125.
https://doi.org/10.1080/02724634.2013.780953

Otero, R.A., O'Gorman, J.P., Hiller, N., O'Keefe, F.R., and Fordyce, R.E. 2016. *Alexandronectes zealandiensis* gen. et sp. nov., a new aristonectine plesiosaur from the lower Maastrichtian of New Zealand. Journal of Vertebrate Paleontology 36:e1054494.
https://doi.org/10.1080/02724634.2015.1054494

Otero, R.A., O'Gorman, J.P., Moisley, W.L., Terezow, M., and McKee, J. 2018. A juvenile *Tuarangisaurus keyesi* Wiffen and Moisley 1986 (Plesiosauria, Elasmosauridae) from the Upper Cretaceous of New Zealand, with remarks on its skull ontogeny. Cretaceous Research 85:214–231. https://doi.org/10.1016/j.cretres.2017.09.007

Otero, R.A. and Soto-Acuña, S. 2021. *Wunyelfia maulensis* gen. et sp. nov., a new basal aristonectine (Plesiosauria, Elasmosauridae) from the Upper Cretaceous of central Chile. Cretaceous Research 118:104651. https://doi.org/10.1016/j.cretres.2020.104651

Otero, R.A., Soto-Acuña, S., and O'Keefe, F.R. 2018. Osteology of *Aristonectes quiriquinensis* (Elasmosauridae, Aristonectinae) from the upper Maastrichtian of central Chile. Journal of Vertebrate Paleontology 38:e1408638. https://doi.org/10.1080/02724634.2017.1408638

Owen, R. 1860. On the orders of fossil and recent Reptilia, and their distribution in time. Reports of the British Association for the Advancement of Science 29:153–166.

Page, R., Ardolino, A., de Barrio, R.E., Franchi, M., Lizuain, A., Page, S., and Silva Nieto, D. 1999. Estratigrafía del Jurásico y Cretácico del Macizo de Somún Curá, provincias de Río Negro y Chubut. In Caminos, R. (ed.), Geología Argentina. SEGEMAR, Buenos Aires, p. 460–488.

Petersen, C.S. 1946. Estudios geológicos en la región del río Chubut Medio. Secretaría de Industria y Comercio, Dirección General de Minas y Geología, Boletín 59, 137 pp.

Ruiz, L., Scasso, R.A., Aberhan, M., Kiessling, W., Bande, A., Medina, F., and Weidemeyer, S. 2005. La Formación Lefipán en el Valle Medio del Río Chubut: ambientes sedimentarios y su relación con la tectónica del Cretácico Tardío–Paleoceno. In: XVI Congreso Geológico Argentino, La Plata, Argentina, Actas 3:231–238.

Sachs, S., Kear, B.P., and Everhart, M.J. 2013. Revised vertebral count in the "longest-necked vertebrate" Elasmosaurus platyurus Cope 1868, and clarification of the cervical-dorsal transition in Plesiosauria. PLoS One, 8(8), e70877. https://doi.org/10.1371/journal.pone.0070877

Sachs, S. and Kear, B.P. 2014. Postcranium of the paradigm elasmosaurid plesiosaurian *Libonectes morgani* (Welles, 1949). Geological Magazine 151:1–17. https://doi.org/10.1017/s0016756814000636

Sachs, S. and Kear, B.P. 2017. Redescription of the elasmosaurid plesiosaurian *Libonectes atlasense* from the Upper Cretaceous of Morocco. Cretaceous Research 74:205–222. https://doi.org/10.1016/j.cretres.2017.02.017

Sander, P.M. 1989. The pachypleurosaurids (Reptilia: Nothosauria) from the Middle Triassic of Monte San Giorgio (Switzerland) with the description of a new species. Philosophical Transactions of the Royal Society of London B 325:561–666. https://doi.org/10.1098/rstb.1989.0103

Sato, T. 2003. *Terminonatator ponteixensis*, a new elasmosaur (Reptilia; Sauropterygia) from the Upper Cretaceous of Saskatchewan. Journal of Vertebrate Paleontology 23:89–103. https://doi.org/10.1671/0272-4634(2003)23[89:tpanes]2.0.co;2

Sato, T., Hasegawa, Y., and Manabe, M. 2006. A new elasmosaurid plesiosaur from the Upper Cretaceous of Fukushima, Japan. Palaeontology 49:467–484. https://doi.org/10.1111/j.1475-4983.2006.00554.x

Sato, T. and Wu, X.C. 2008. A new Jurassic pliosaur from Melville Island, Canadian Arctic Archipelago. Canadian Journal of Earth Sciences 45:303–320. https://doi.org/10.1139/e08-003

Sato, T., Wu, X.C., Tirabasso, A., and Bloskie, P. 2011. Braincase of a polycotylid plesiosaur (Reptilia: Sauropterygia) from the Upper Cretaceous of Manitoba, Canada. Journal of Vertebrate Paleontology 31:313–329. https://doi.org/10.1080/02724634.2011.550358

Scasso, R.A., Aberhan, M., Ruiz, L., Weidemeyer, S., Medina, F.A., and Kiessling, W. 2012. Integrated bio- and lithofacies analysis of coarse-grained, tide-dominated deltaic environments across the Cretaceous/Paleogene boundary in Patagonia, Argentina. Cretaceous Research 36:37–57. https://doi.org/10.1016/j.cretres.2012.02.002

Schumacher, G.H. 1973. The head muscles and hyolaryngeal skeleton of turtles and crocodilians. In Gans, C. and Parsons, T.S. (eds.), Biology of the Reptilia, vol. 4. Academic Press, London, p. 101–199.

Schumacher, B.A. and Martin, J.E. 2016. *Polycotylus latipinnis* Cope (Plesiosauria, Polycotylidae), a nearly complete skeleton from the Niobrara Formation (early Campanian) of southwestern South Dakota. Journal of Vertebrate Paleontology 36:e1031341. https://doi.org/10.1080/02724634.2015.1031341

Schwenk, K. 1986. Morphology of the tongue in the tuatara, *Sphenodon punctatus* (Reptilia: Lepidosauria), with comments on function and phylogeny. Journal of Morphology 188:129–156. https://doi.org/10.1002/jmor.1051880202

Schwenk, K. 2000. Feeding in lepidosaurs. In Schwenk, K. (ed.), Feeding: Form, Function, and Evolution in Tetrapod Vertebrates. Academic Press, San Diego, p. 175–291. https://doi.org/10.1016/b978-012632590-4/50009-5

Serratos, D.J., Druckenmiller, P., and Benson, R.B. 2017. A new elasmosaurid (Sauropterygia, Plesiosauria) from the Bearpaw Shale (Late Cretaceous, Maastrichtian) of Montana demonstrates multiple evolutionary reductions of neck length within Elasmosauridae. Journal of Vertebrate Paleontology 37:e1278608. https://doi.org/10.1080/02724634.2017.1278608

Smith, A.S. and Vincent, P. 2010. A new genus of pliosaur (Reptilia: Sauropterygia) from the Lower Jurassic of Holzmaden, Germany. Palaeontology 53:1049–1063 https://doi.org/10.1111/j.1475-4983.2010.00975.x

Storrs, G.W. 1997. Morphological and taxonomic clarification of the genus Plesiosaurus. In Ancient Marine Reptiles, pp. 145-190, Academic Press. https://doi.org/10.1016/b978-012155210-7/50010-7

Tanner, W.W. and Avery, D.F. 1982. Buccal floor of reptiles, a summary. The Great Basin Naturalist 42:273–349.

Turner, J. 1983. Descripción Geológica de la Hoja 44d, Colán Conhüé, Provincia del Chubut. Servicio Geológico Nacional, Boletín N° 197, 92 pp.

Vajda, V. and Raine, J.I. 2010. A palynological investigation of plesiosaur-bearing rocks from the Upper Cretaceous Tahora Formation, Mangahouanga, New Zealand. Alcheringa: An Australasian Journal of Palaeontology 34:359–374. https://doi.org/10.1080/03115518.2010.486642

Vincent, P., Bardet, N., Suberbiola, X.P., Bouya, B., Amaghzaz, M., and Meslouh, S. 2011. *Zarafasaura oceanis*, a new elasmosaurid (Reptilia: Sauropterygia) from the Maastrichtian phosphates of Morocco and the palaeobiogeography of latest Cretaceous plesiosaurs. Gondwana Research 19:1062–1073. https://doi.org/10.1016/j.gr.2010.10.005

Wang, W., Li, C., Scheyer, T.M., and Zhao, L. 2019. A new species of *Cyamodus* (Placodontia, Sauropterygia) from the early Late Triassic of south-west China. Journal of Systematic Palaeontology 17:1457–1476. https://doi.org/10.1080/14772019.2018.1535455

Welles, S.P. and Gregg, D.R. 1971. Late Cretaceous marine reptiles of New Zealand. Records of the Canterbury Museum 9:1–111.

Welles, S.P. 1943. Elasmosaurid plesiosaurs with description of new material from California and Colorado. Memoirs of the University of California 13:125–234.

Welles, S.P. 1949. A new elasmosaur from the Eagle Ford Shale of Texas. Part I. Systematic description. Fondren Science Series 1:1–28.

Welles, S.P. 1952. A review of the North American Cretaceous elasmosaurs. University of California Publications in Geological Sciences 29:1–144.

Welles, S.P. 1962. A new species of elasmosaur from the Aptian of Colombia and a review of the Cretaceous plesiosaurs. University of California Publications in Geological Sciences 44:1–96.

Wiffen, J. and Moisley, W.L. 1986. Late Cretaceous reptiles (Families Elasmosauridae and Pliosauridae) from the Mangahouanga Stream, North Island, New Zealand. New Zealand Journal of Geology and Geophysics 29:205–252. https://doi.org/10.1080/00288306.1986.10427535

Williston, S.W. 1903. North American plesiosaurs, Part 1. Field Columbian Museum Publication (Geology) 73:1–77. https://doi.org/10.5962/bhl.title.3497

Williston, S.W. 1908. North American plesiosaurs: *Trinacromerum*. Journal of Geology 16:715–736. https://doi.org/10.1086/621573

Xu, G.H., Shang, Q.H., Wang, W., Ren, Y., Lei, H., Liao, J.L., and Li, C. 2023. A new long-snouted marine reptile from the Middle Triassic of China illuminates pachypleurosauroid evolution. Scientific Reports 13:16. https://doi.org/10.1038/s41598-022-24930-y

Zinsmeister, W.J. 1979. Biogeographic significance of the late Mesozoic and early Tertiary molluscan faunas of Seymour Island (Antarctic Peninsula) to the final breakup of Gondwanaland. Ohio State University, Institute of Polar Studies, pp. 349–355.

Zverkov, N.G., Averianov, A.O., and Popov, E.V. 2018. Basicranium of an elasmosaurid plesiosaur from the Campanian of European Russia. Alcheringa: An Australasian Journal of Palaeontology 42:528–542. https://doi.org/10.1080/03115518.2017.1302508

SUPPLEMENTARY MATERIAL

SUPPLEMENTARY MATERIAL 1. Data set comprising *Tuarangisaurus keyesi* (holotype NPC CD 425 and NPC CD 426) and the specimen (MPEF-PV 12001) as separate scorings.
(Available for download at https://palaeo-electronica.org/content/2026/5903-first-record-of-tuarangisaurus-from-argentina)

SUPPLEMENTARY MATERIAL 2. Data set comprising *Tuarangisaurus keyesi* with combined scores (NPC CD 425 + NPC CD 426 + MPEF-PV 12001).
(Available for download at https://palaeo-electronica.org/content/2026/5903-first-record-of-tuarangisaurus-from-argentina)